

SWEET BRIAR COLLEGE



3 2449 0468502 2

Digitized by the Internet Archive
in 2010 with funding from
Lyrasis Members and Sloan Foundation

<http://www.archive.org/details/howtoutilizecost00ciri>

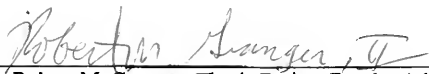
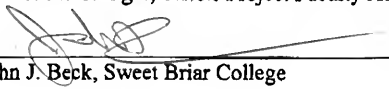
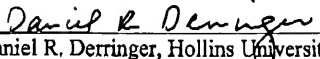
**HOW TO UTILIZE CO₂?
STUDIES OF NOVEL CO₂ REDUCTION CATALYSTS**

**A Senior Honors Thesis Research in the
Department of Chemistry
Submitted to the Honors Committee of
Sweet Briar College**

By Ana Ciric

Defended and Approved 28 April 2005

Awarded High Honors

	5/11/05
Dr. Robert M. Granger, Thesis Project Faculty Advisor, Sweet Briar College	Date
	10 MAY 05
Dr. John J. Beck, Sweet Briar College	Date
	5-6-2005
Dr. Daniel R. Derringer, Hollins University	Date

To all second-floor Guionites

ACKNOWLEDGEMENTS

First and foremost, I would like to thank the entire Chemistry Department for their continuous support and encouragement during the past four years. Sweet Briar College has made me a well-rounded person, but moreover the Department has made me the person I want to be – ambitious, diligent, persistent, patient, hard-working, and life-long “chem nerd.” Thank you for teaching me many little pieces of a big puzzle that are finally coming together. Thank you for allowing me to reach my potential and for preparing me for a new start in graduate school. I would especially like to thank my advisor Dr. Rob Granger for drawing me into the field of chemistry and having confidence in me; allowing me to work in your lab after my freshman year was slightly frightening but awarding!

I would also like to acknowledge the Honors Summer Research Program for funding my research experience for the summers 2003 and 2004, as well as the Jeffress Memorial Trust for funding the research.

And last, but not least, I would like to thank my friends and family for their endless support and encouragement in the most difficult days, and for making me realize that every little bump on the road can be overcome.

TABLE OF CONTENTS

Page

Abstract.....	iii
Publication.....	
List of Figures.....	iv
List of Schemes.....	iv
Section 1: Introduction.....	1
Section 1.1: Why CO ₂ ?.....	1
Section 1.2: Activation of CO ₂ and Carbon-Carbon Bond Formation.....	2
Section 1.3: Synthesis of a Carbon-Carbon Bond Forming CO ₂ Reduction Catalyst.....	6
Section 2: Project Objectives.....	8
Section 3: Chemicals and Equipment.....	9
Section 4: Experimental.....	10
Section 4.1: Synthesis of [Pt(dpk) ₂ Cl ₂] ²⁺	10
Section 4.2: Crystal Chamber set-up.....	10
Section 4.3: Electrocatalytic Reduction of [Pt(dpk) ₂ Cl ₂] ²⁺	10
Section 4.4: Bulk Cell Electrolysis Experiments.....	11
Section 4.5: Product Extraction Procedures.....	12
Section 4.6: Esterification of a Commercially-Obtained <i>trans</i> -1,2-cyclohexanedicarboxylic acid.....	13
Section 4.7: Esterification of a Commercially-Obtained Oxalic Acid.....	13
Section 4.8: Synthesis of Poly-dpk Catalyst.....	13
Section 5: Results and Discussion.....	14
Section 5.1: Electrocatalytic Reduction of [Pt(dpk)Cl ₄].....	14
Section 5.2: Spectroscopic Characterization of [Pt(dpk) ₂ Cl ₂] ²⁺	18
Section 5.3: Carbon-Carbon Bond Formation.....	19
Section 5.4: Most Recent Exploration of our [Pt(dpk) ₂ Cl ₂] ²⁺	23
Section 6: Conclusion.....	25
Section 7: Future Research.....	25
References.....	26
Appendix A: X-ray Crystallographic Data	
Appendix B: GC/MS, NMR, and IR spectra	

ABSTRACT

Ana Ciric

Department of Chemistry, Sweet Briar College, Sweet Briar VA 24595

The electrochemical reduction of CO₂ by transition metal catalysts has acquired much attention over the past two decades.¹ The reduction of CO₂ is the first step in the formation of carbon-carbon bonds using CO₂ as a feed stock. Due to the fact that CO₂ is thermodynamically stable and kinetically inert, the activation of CO₂ is difficult, and the efficient use of CO₂ as a synthetic feed stock has remained a challenge.¹ We report the homogeneous electrocatalytic reduction of CO₂ by tetrachloro(di-2-pyridyl ketone)platinum(IV), [Pt(dpk)Cl₄]. Furthermore, reduction occurs at nearly a full volt lower potential than previously reported CO₂ electrocatalysts. Herein, we report the synthesis, x-ray structures and spectroscopic characterization of both the hydrated and anhydrous forms of [Pt(dpk)Cl₄]. Also, the synthesis, characterization and x-ray crystal structure of the hydrated form of dichloro bis(di-2-pyridyl ketone platinum (IV), [Pt(dpk)₂Cl₂]²⁺ catalyst is presented. Along with some preliminary CO₂ reduction data, several initial electrochemical experiments, chemical trapping experiments, and labeling studies have been performed confirming the possible development of a system in which CO₂ molecules are simultaneously reduced, ultimately resulting in the formation of carbon-carbon bonds.

A NEW *CIS*-PLATIN ANALOG? THE SYNTHESIS, CHARACTERIZATION, SELECTIVE CYTOTOXICITY AND DNA BINDING STUDIES OF TETRACHLORO(1,10-PHENANTHROLINE-5,6-DIONE) PLATINUM(IV); X-RAY STRUCTURE ANALYSIS OF DICHLORO(1,10-PHENANTHROLINE-5,6-DIONE) PLATINUM(II)

Robert M. Granger†, II; Robin Davies‡; Kimberly Anne Wilson; Erica Kennedy; Bricanne Vogler, Yen Nguyen, Eric Mowles, Regan Blackwood, Ana Ciric, & Peter S. White*

Departments of Chemistry & Biology, Sweet Briar College, Sweet Briar, Virginia, 24595

Abstract

We report on the synthesis, characterization, selective cytotoxicity and DNA binding of the molecule Tetrachloro(1,10-phenanthroline-5,6-dione)platinum(IV) [Pt(dione)Cl₄]. Additionally, we report the X-ray structure of Dichloro(1,10-phenanthroline-5,6-dione)platinum(II), [Pt(dione)Cl₂]. This X-ray structure shows the first example of the dione ligand chelated to a platinum(II) center as a diimene rather than the preferred quinone binding mode. The electrochemical behavior of [Pt(dione)Cl₂] is rather complex and some initial studies are presented within. The energy of the electronic transitions within [Pt(dione)Cl₂] show a strong solvent dependence with some evidence of the formation of the hydroquinone in protic solvents. Cell culture studies of [Pt(dione)Cl₂] conducted on normal (WI-38) and transformed cells (G-401) showed a remarkable degree of selectivity cytotoxicity. DNA binding studies comparing [Pt(dione)Cl₂] and *cis*-platin were conducted with poly(dG-dC)-poly(dG-dC), poly(dG-dG)-poly(dC-dC), and poly(dA-dT)-poly(dA-dT). These studies indicates a DNA binding mechanism for [Pt(dione)Cl₂] that is uniquely different than that of *cis*-platin.

Keywords:

Introduction

Molecules of the type [M(*N-N*)₃]ⁿ⁺ where M = transition metal and *N-N* = a diimene ligand of the type 2,2'-dipyridine (dipy) or 1,10-phenanthroline (phen) have been thoroughly studied both for their extensive photochemistry (1), as well as, for their utility as probes of DNA structure (2-30).

The photochemistry of [M(*N-N*)₃]ⁿ⁺ type molecules was heavily studied during the early 1970's with the hopes of finding a photolytic catalyst for the disproportionation of water (15) and beginning in the early 1980's, researchers began examining the interactions of octahedrally coordinated diimene complexes of copper, nickel, zinc, iron, cobalt, chromium, rhodium, osmium, and especially ruthenium with DNA (2-30). In many cases, these complexes had been shown to bind to

DNA by one or more mechanisms (electrostatics, groove binding or intercalation), and in some cases, the binding was regioselective (7,8;10-12). Therefore, there was the hope that these complexes would be useful as probes of DNA structure.

Stemming from this body of research, investigations into the synthesis and characterization of 1,10-phenanthroline-5,6-dione (dione) complexes with several different transition metals [Ru (31-37), Fe (32,33,38), Co (32,33,36,38;39), Cu (32,38), Cr (33), Ni (33,35;38), Zn (38), Re (33), Pd (37), Pt (36), and Os (32;35)] have been reported in the literature. The chelating dione ligand can bind to the metal center either as a diimene or as a catecholate (quinone) (35-38,40;41). The recent popularity of the dione ligand results from both its unique electrochemical behavior as a quinone ligand (32, 33,35,38;42-48) and from its versatility as a synthetic

† Corresponding author to whom questions regarding synthesis, characterization, and DNA binding studies should be addressed: Sweet Briar College Department of Chemistry, Sweet Briar, VA 24595; tel: 434-381-6403; fax: 434-381-6488; email: rgranger@sbc.edu.

‡ Corresponding author to whom questions regarding cell culture studies should be addressed: Sweet Briar College Department of Biology, Sweet Briar, VA 24595; tel: 434-381-6196; fax: 434-381-6488; email: davies@sbc.edu.

* Corresponding author to whom questions regarding X-ray structure should be addressed: Department of Chemistry, University of North Carolina, Chapel Hill, NC 27599

precursor for phenazine-type ligand syntheses, such as dipyrro[3,2-a:2',3'-c]phenazine (dppz) (49). These dppz type ligands have been shown to provide a means to intercalative DNA probes with interesting photophysical properties (2,3,34,39;50-56). It should also be noted that quinones have been extensively studied as antitumor agents (57).

Although many metal complexes have been used as DNA probes (2-30), only compounds of the platinum family are widely used medicinally as chemotherapeutic agents (58;59). For example, *cis*-platin (*cis*-diamminedichloroplatinum) is widely used alone or in combination with other chemotherapeutic drugs in the treatment of several aggressive cancers, including ovarian, lung, testicular, and bladder carcinomas (58;59). Unfortunately, resistance to *cis*-platin often develops and the drug itself is toxic to the patient, with the kidneys, gastrointestinal tract, bone marrow, and nervous system all experiencing distress resulting from treatment and not all tumors respond to *cis*-platin (58;59), so there is of course the hope that new drugs might be found which would be effective against *cis*-platin-resistant tumors.

We report the synthesis and spectroscopic characterization of tetrachloro(1,10-phenanthroline-5,6-dione)platinum(IV); [Pt(dione)Cl₄] along with the X-ray structure of the reduced form dichloro(1,10-phenanthroline-5,6-dione)Pt(II); [Pt(dione)Cl₂]. Additionally, we present some very encouraging preliminary cytotoxicity studies that demonstrate a high degree of selectivity.

Last, we have conducted preliminary DNA binding studies that show the effect that [Pt(dione)Cl₄] has on the electrophoretic migration rate poly(dG-dC)-poly(dG-dC) is five times stronger than the effect *cis*-platin has on the electrophoretic migration rate of poly(dG-dC)-poly(dG-dC) (59;60).

Experimental Section

Materials

1,10-phenanthroline-5,6-dione (dione) was synthesized by the method of Yamada *et al.* (39) as modified by Paw and Eisenberg (36). Potassium hexachloroplatinate, K₂PtCl₆, was purchased from Aldrich Chemical Company and used as received. Ultrapure (eighteen megaohm) water was generated

in our labs using the Modulab Modupure Plus system.

Synthesis of Tetrachloro(1,10-phenanthroline-5,6-dione)platinum(IV), [Pt(dione)Cl₄]

A mass of 0.1640 g K₂PtCl₆ (3.37×10^{-4} mol) and a mass of 0.0715 g of the dione ligand (3.37×10^{-4} mol) were each separately dissolved into 25 mL of ultrapure water. The two solutions were then combined and allowed to stir at room temperature overnight. The compound [Pt(dione)Cl₄] precipitates as a yellow/orange micro-crystalline solid and can be recrystallized from Acetone/Ether or DMSO/Ether.

Spectroscopy

The FT-IR spectrum was collected using a 4020 Galaxy Series Mattson FT-IR as a KBr pellet. UV-vis spectra were recorded using a Hewlett-Packard 8452A diode array spectrophotometer. NMR spectra were measured on a JEOL ECX 400 spectrometer in CH₃CN and referenced with TMS.

Electrochemical Experiments

All electrochemical experiments were conducted using a Princeton Applied Research Versastat. The working electrode used for cyclic voltammetry was a 3 mm diameter platinum electrode purchased from Bio-Analytical Systems (BAS). The electrode was polished using 0.5 micron alumina. The counter electrode consisted of a platinum wire. The reference was Ag/AgCl "no-leak" purchased from Cypress Systems (Part # 66-EE009). Acetonitrile used for these experiments was dried over 3Å sieves. TBAP was purchased from Aldrich Chemical Company and used as received.

X-ray analysis of dichloro(1,10-phenanthroline-5,6-dione)platinum(II), [Pt(dione)Cl₂]

Crystals suitable for X-ray analysis were obtained by slow diffusion from DMSO/Ether. It should be noted that the compound [Pt(dione)Cl₄] was dissolved in DMSO yet the crystal obtained was [Pt(dione)Cl₂]. We speculate that the DMSO promoted the reductive elimination of two chlorides. The intensity data were collected on a Bruker SMART 1K diffractometer, using the omega scan mode (60;61). The h,k,l ranges used during structure solution and refinement are: H_{min,max}-12,10; K_{min,max}-26, 26; L_{min,max}-9, 8; No. of reflections measured = 6530; No. of unique reflections = 2268;

No. of reflections with $I_{\text{net}} > 2.5\sigma(I_{\text{net}}) = 2198$: Merging R-value on intensities = 0.028. Correction was made for absorption using SADABS. Ratio of minimum to maximum apparent transmission: 0.408232. Additional spherical absorption correction applied with $\mu^*r = 0.6750$.

Details of the last least squares cycle; 35 atoms, 207 parameters, Full-matrix on Fo, Counter wts (k 0.000500). The residuals are as follows: Significant reflections: 2198, $R_f = 0.028$, $R_w = 0.035$. All reflections: 2268, $R_f = 0.029$, $R_w = 0.036$. Included reflections: 2198, $R_f = 0.028$, $R_w = 0.035$ $G_{\text{of}} = 1.1595$ where $R_f = \text{Sum}(\text{Fo}-\text{Fc})/\text{Sum}(\text{Fo})$, $R_w = \sqrt{\text{Sum}(\text{w}(\text{Fo}-\text{Fc})^2)/\text{Sum}(\text{wFo}^2)}$ and $G_{\text{of}} = \sqrt{\text{Sum}(\text{w}(\text{Fo}-\text{Fc})^2)/(\text{No. of reflections} - \text{No. of params.})}$. The maximum shift/sigma ratio was 0.000. Last D-map: Minimum density -1.150e/A**3, Maximum density 1.110e/A**3. Secondary ext. coeff. = 0.2207microns, sigma = 0.0257. Cell dimensions were obtained from 870 reflections with 2Theta angle in the range 10.00-140.00 degrees.

Cell Culture. Two normal human cell lines, WI-38 (ATCC # CCL-75) and Hs578Bst (ATCC # HTB-125), and two transformed human cell lines, G-401 (ATCC # CRL-1441) and Hs 578T (ATCC # HTB-126), were purchased from the American Type Culture Collection. The WI-38 cells were grown in 90% Minimal Essential Medium Eagle supplemented with 10% fetal bovine serum (FBS). G-401 cells were maintained in 90% McCoy's 5a Medium with 10% FBS. The Hs578Bst and Hs 578T cell lines were obtained from a breast tissue biopsy of a single individual. These cells were maintained in 90% Dulbecco's Modified Eagle Medium (DMEM) supplemented with 10% FBS, 10 $\mu\text{g/mL}$ bovine insulin, and 30 ng/mL human epidermal growth factor (EGF). Media components were purchased from GIBCO/Invitrogen. Cultures were grown at 37 °C in an atmosphere of 5% CO₂.

Cytotoxicity Assay

Cells were plated in 96-well tissue culture plates and allowed to grow for 24-72 hours prior to treatment. A stock solution of 1 mM [Pt(dione)Cl₂] in DMSO was prepared and diluted ten-fold in culture medium. Cells were supplemented with one-tenth volume of this 0.1 mM stock resulting in a final concentration of 1% DMSO and 10 mM [Pt(dione)Cl₂]. Since the x-ray data suggests that the

Pt(IV) center is reduced to Pt(II) in DMSO, it is likely that the active form of our drug is [Pt(dione)Cl₂].

Following a 48 hour incubation period, 3-[4,5-dimethylthiazol-2-yl]-2,5-diphenyl tetrazolium bromide (MTT) was added to a final concentration of 0.5 mg/mL. Cells were then incubated for 2-4 hours, during which time metabolically active cells reduced the MTT to an insoluble blue formazan. The culture medium was removed and the formazan was solubilized with DMSO. Absorbance at 540 nm was determined using a Tecan Spectra Shell microplate reader. Each plate included untreated control wells and 1% DMSO control wells. Statistical analyses of results were conducted using the SuperANOVA from Abacus Concepts.

DNA Binding Studies

High melting agarose, Trizma Base and Ethidium Bromide were purchased from Aldrich Chemical Company. Glacial acetic acid was purchased from VWR. EDTA was purchased from IBI (Subsidiary of Eastman Kodak Company). Poly(dG-dC)-poly(dG-dC), poly(dG-dG)-poly(dC-dC), and poly(dA-dT)-poly(dA-dT) DNA were purchased from Amersham Biosciences and I-DNA HindIII digest was purchased from New England Biolabs. Concentrated buffer (buffer #1) containing 2.0 M (tris[hydroxymethyl]aminomethane) (TrisBase), 1M acetic acid and 0.05 M EDTA was made by dissolving 48.4 grams of trisbase, 11.42 mL of glacial acetic acid, and 20 mL of 0.5 M EDTA into 200 mL of ultrapure water. The concentrated buffer was diluted by taking 20 mL of buffer #1 and diluting it to 1 liter (buffer #2 = 0.02M TrisBase, 0.01M acetic acid & 0.0005M EDTA). Running buffer for the control gels (buffer #3) was made by dissolving 0.210 g of NaCl into 200 mL of buffer #2 and then adjusting the pH of the buffer to 7 using glacial acetic acid. Running buffer for the test gels was made in the same manner as buffer #3 with the addition of 10 mM drug. Gels for both the control and test runs were made by taking 0.4 g of agarose and dissolving that into 40 mL of the appropriate running buffer. Both the control gel and the test gel were run at 125 V/m for 1 hour and 20 minutes, stained in ethidium bromide, and destained in 1 mM MgSO₄. The change in DNA migration rate was calculated as a % change relative to a control gel and represents a retardation of electrophoretic mobility in the presence of drug.

Results and Discussion

Structure Analysis & X-ray Crystallography

The compound $[\text{Pt}(\text{dione})\text{Cl}_2]$ cocrystallized with one DMSO molecule to produce an empirical formula of $\{\text{PtCl}_2\text{C}_{14}\text{H}_{12}\text{N}_2\text{O}_3\text{S}\}$. The crystal was monoclinic, Cc with $a = 9.9445(11)$, $b = 22.906(3)$, $c = 7.5534(9)$, $\beta = 111.735(1)$, and a volume of $1598.3(3)\text{\AA}^3$ (62). Crystal dimensions = $0.10 \times 0.07 \times 0.03$ mm. $\text{FW} = 554.31$, $Z = 4$, $F(000) = 1037.18$. $D_{\text{calc}} = 2.304\text{Mg}\cdot\text{m}^{-3}$, $\mu = 20.24\text{mm}^{-1}$, $\lambda = 1.5418\text{\AA}$, $2\theta(\text{max}) = 140.0$.

The first platinum (II)-dione compound was published by Balch in 1975 (37). In that paper, the compound $[\text{Pt}(\text{dione})(\text{PPh}_3)_2]$ was described and characterized by elemental analysis and spectroscopic means only. Furthermore, Balch concluded that the dione ligand chelated as a quinone, binding to the platinum through the α -oxygen instead of through the α -diimenes. This conclusion was based upon the fact that the carbonyl stretch was absent in the infrared spectrum. In contrast, Balch also concluded that palladium(II) does not bind to the dione ligand as a quinone but rather binds through the α -diimenes to form $[\text{Pd}(\text{dione})\text{Cl}_2]$. This conclusion was supported by the appearance of the carbonyl stretch in the infrared spectrum. In 1991, Pierpont (40) reported a bimetallic complex of the quinone-dione ligand in which a palladium(II) had chelated through the α -diimene system and a platinum(II) had chelated through the α -oxygen system. In 1997, Eisenberg (36) studied this system further. He noted a similar coordination preference for platinum(II) for the quinone-dione ligand and he made several platinum(II) compounds containing both the quinone-dione ligand and di-*tert*-butyldipyridine. In all cases, Eisenberg noted that platinum(II) bound to the quinone-dione ligand through the α -oxygen.

However, the observed preference for binding to the α -oxygen in dione by platinum(II) is not a result of an inherent instability of platinum(II) diimenes. In fact, Gray *et al.* reported the synthesis of dichloro(2,2'-dipyridine)platinum(II) $[\text{Pt}(\text{dipy})\text{Cl}_2]$ in 1996, clearly demonstrating the ability of platinum(II) to bind to a diimene ligand through the α -diimenes (63). It is curious to note that given the choice, platinum(II) prefers to bind to the quinone-dione ligand as a quinone yet palladium(II) prefers

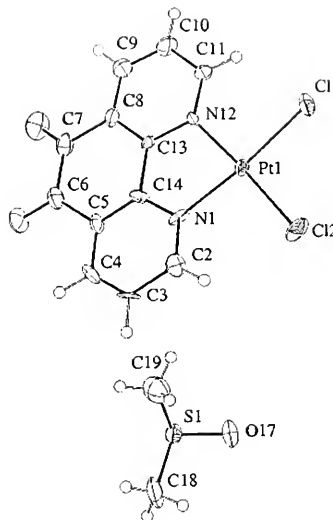


Figure1. ORTEP diagram for $[\text{Pt}(\text{dione})\text{Cl}_2]$ showing 95% confidence ellipsicals.

to bind through the α -diimenes. We report the first observation of a platinum(II) center bound to 1,10-phenanthroline-5,6-dione (dione) through the α -diimene system $[\text{Pt}(\text{dione})\text{Cl}_2]$.

In this case, the dione ligand was first coordinated to a platinum(IV) center prior to reduction by DMSO to platinum(II). We speculate that this is the reason for the reversal of the dione-Pt(II) binding mode (64-66).

An ORTEP diagram of $[\text{Pt}(\text{dione})\text{Cl}_2]$ can be seen in Figure 1 and a table comparing selected bond angles and bond lengths of $[\text{Pt}(\text{dione})\text{Cl}_2]$ to that of $[\text{Pt}(\text{dipy})\text{Cl}_2]$ (63) can be seen in Table 1. In light of the fact that the literature precedence for binding of the dione ligand to Pt(II) favors binding through the α -oxygen, it is curious to note how similar the structures of $[\text{Pt}(\text{dione})\text{Cl}_2]$ is to that of $[\text{Pt}(\text{dipy})\text{Cl}_2]$.

Spectroscopy

The Infrared spectrum of $[\text{Pt}(\text{dione})\text{Cl}_4]$ is seen in Figure 2. The ketone functional group is clearly seen in the IR at 1703.99 cm^{-1} as are other stretches associated with the fused poly-aromatic ring system. **Table 1.** Bond lengths (\AA) and bond angles ($^\circ$) for $[\text{Pt}(\text{dione})\text{Cl}_2]$ compared to the analogous bond

lengths (Å) and bond angles (deg) for [Pt(dipy)Cl₂] (Gray et al. (63)).

Cl ₁ -Pt-Cl ₂	89.93°	89.12°
N ₁ -Pt-N ₁₂	81.23°	86.14°
N ₁₂ -Pt-Cl ₁	93.79°	95.37°
N ₁ -Pt-Cl ₂	95.12°	95.37°
Cl ₂ -Pt-N ₁₂	175.51°	175.51°
Cl ₁ -Pt-N ₁	174.41°	175.51°
Pt-Cl ₁	2.290°	2.302°
Pt-Cl ₂	2.291°	2.302°
Pt-N ₁₂	2.009°	2.009°
Pt-N ₁	2.049°	2.009°

Figure 2. Infrared Spectrum of [Pt(dione)Cl₂] taken as a KBr pellet

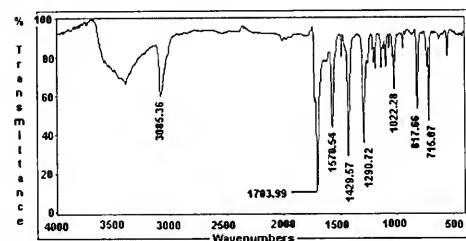


Figure 3 shows a UV-visible spectrum of [Pt(dione)Cl₂] as well as the UV-visible spectrum of the free dione ligand (not coordinated to Pt(IV)). Both spectra were taken in acetonitrile. Two excitation bands are seen for the free ligand (Figure 3B), one at 300 nm and another at 370 nm.

Table 2 provides absorption maxima and molar absorptivities (ϵ) for free dione in various solvents ranging in polarity. With the exception of cyclohexane, all of these solvents show a band at approximately 300 nm. For ethanol, acetonitrile and water, we see the appearance of a lower energy band that has an energy that is strongly solvent dependent yet does not have a clear hyper nor hypochromicity. It is quite possible that this band is due to the formation of the hydroquinone in the protic solvents ethanol and water and trace water in acetonitrile. Due to the hydrophobicity of cyclohexane, we would not expect to see the formation of the hydroquinone and the basicity of DMSO would likewise inhibit the formation of the hydroquinone. This is further substantiated by the observation that we see a higher energy band in cyclohexane (254 nm) and DMSO (262 nm) that red shifts as the solvent polarity is

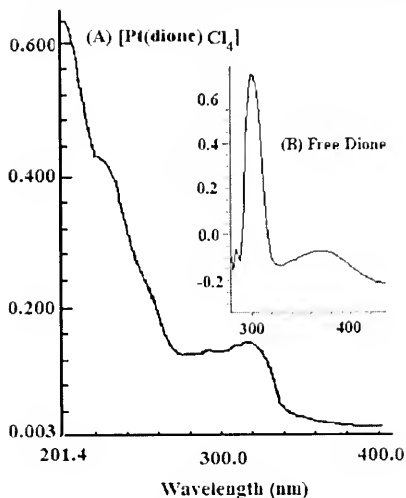


Figure 3. (A) Ultraviolet-visible spectrum of [Pt(dione)Cl₂] in dry acetonitrile. (B) Ultraviolet-visible spectrum of free 1,10-phenanthroline-5,6-dione (dione) in dry acetonitrile.

Table 2. Absorption Maxima and Molar Absorptivities for free 1,10-phenanthroline-5,6-dione (dione) in Various Solvents.

Solvent	Snyder Polarity Index (67)	λ_{\max} (nm)(ϵ , cm ² M ⁻¹)
Cyclohexane	0	254 (4214.6), 282 sh
Ethanol	5.2	--- 300 (6143.4), 358 sh
Acetonitrile	6.2	--- 300(6482.4), 370 (1050.9)
DMSO	6.5	262, 294 sh
Water	9	--- 298 (5278.0), 364 sh

Table 3. Absorption Maxima and Molar Absorptivities for [Pt(dione)Cl₂] in Various Solvents.

Solvent	Snyder Polarity Index (67)	λ_{\max} (nm)(ϵ , cm ² M ⁻¹)
Ethanol	5.2	--- 308 (10999), 320 sh
Acetonitrile	6.2	227 (46500), 290.5 (14500), 317.5 (16200)
DMSO	6.5	264, 294

increased. This is most likely due to an $n-\pi^*$ transition occurring from the lone pairs of the dione (non-hydroquinone) system.

The UV-visible spectrum of $[\text{Pt}(\text{dione})\text{Cl}_4]$ is also shown in Figure 3. Table 3 provides absorption maxima and molar absorptivities (ϵ) for $[\text{Pt}(\text{dione})\text{Cl}_4]$ in various solvents ranging in polarity. Again we suggest that there may be a strong contribution from the hydroquinone in ethanol as evidenced by the low energy band at 320 nm in ethanol and the absence of that peak in DMSO.

Electrochemistry

Acetonitrile solutions containing $5.38 \times 10^{-5}\text{M}$ (saturated) $[\text{Pt}(\text{dione})\text{Cl}_4]$ and 0.40M TBAP were used to explore the redox chemistry of $[\text{Pt}(\text{dione})\text{Cl}_4]$. In all cases, the initial potential was +0.5 V vs Ag/AgCl.

Several interesting features are seen in the cathodic sweep. For the sake of this discussion we will make reference to these peaks using the potentials from scan (B) in Figure 4.

The first cathodic peak is seen at +19 mV and its potential does not vary with scan rate. Also, the relative magnitude of this peak seems to remain fairly constant with scan rate however it does get "swallowed up" by the larger peak at -121 mV as the scan rate is decreased. The second cathodic peak can be seen at -121 mV. Like the peak at +19 mV, the peak at -121 mV does not vary with scan rate. However, at fast scan rates this peak's magnitude is greatly diminished. We also ran a scan at 2000 mV/s (not shown) and obtained a scan that was essentially identical to scan (A). We speculate that the peak at -121 mV is actually the result of a reduction followed by a fast chemical change that then results in a second reduction. At faster scan rates we beat the kinetics of the chemical change and thus do not see the contribution from the second reduction at -121 mV. The third cathodic peak (-473 mV) is more complex. At the slower scan rate of 10 mV/s, this peak is resolved into two peaks, one at -502 mV and another at -683 mV. At the faster scan rate of 1000 mV/s, this peak again collapses into a single peak but its potential is shifted negative by 31 mV.

There are also several interesting features seen in the anodic sweep. The first anodic peak seen in sweep (B) occurs at -382 mV. The position of this peak shifts to more positive values as the scan rate is increased. The second anodic peak seen in scan B is seen at -1 mV. The position of this peak shifts to more negative

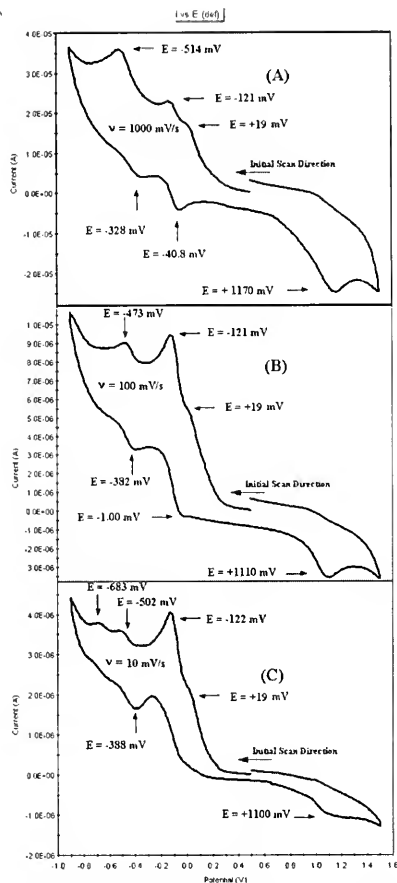


Figure 4. Cyclic Voltammograms of a saturated acetonitrile solution of $[\text{Pt}(\text{dione})\text{Cl}_4]$ with 0.4 M TBAP. Initial potential was 0.50 V vs Ag/AgCl. Arrow indicates the original direction of the scan. (A) Scan rate of 1000 mV/s. (B) Scan rate of 100 mV/s. (C) Scan rate of 10 mV/s.

potentials when the scan rate is increased to 1000 mV/s (see Scan A) and disappears entirely when the scan rate is slowed to 10 mV/s (see Scan C). Also, this peak does not appear at all if the initial direction of the cyclic voltammogram is reversed (see Figure 5). Clearly it is an oxidation of a product produced during the original cathodic sweep. The last anodic peak is seen at +1110 mV. The behavior of this peak is similar to the anodic peak at -1 mV. It also shifts to more positive values when the scan rate is

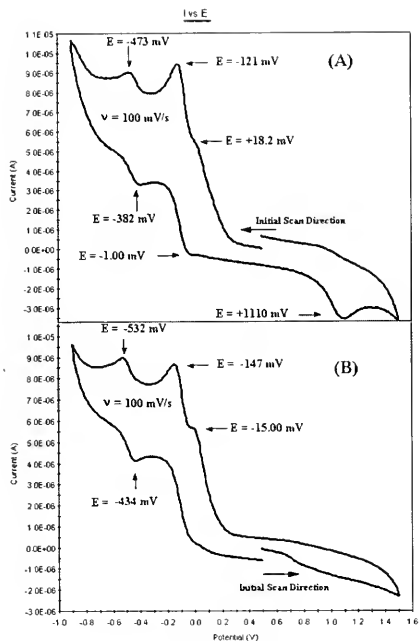


Figure 5. Cyclic Voltammograms of a saturated acetonitrile solution of $[\text{Pt}(\text{dione})\text{Cl}_4]$ with 0.4 M TBAP. Initial potential was 0.50 V vs Ag/AgCl. Arrow indicates the original direction of the scan. (A) Initial potential sweep in the cathodic (negative) direction. (B) Initial potential sweep in the anodic (positive) direction.

increased to 1000 mV and its magnitude decreased dramatically when the scan rate was slowed to 10 mV/s. It is also absent when the initial direction of the voltammogram is reversed (see Figure 5). Again we conclude that it is an oxidation of a product produced during the original cathodic sweep.

Figure 5 shows the affect of changing the original sweep direction. Both scans were conducted at 100 mV/s. When comparing scan A to scan B, we see that two of the anodic peaks from A (-1 mV and +1110 mV) are absent in B. We conclude that these two peaks are the oxidation of products produced during an initial cathodic sweep. With the exception of these two peaks, the remainder of the anodic CV looks similar to that of the cathodic CV.

Figure 6 shows a cyclic voltammogram of the free dione ligand. We clearly see only one redox event

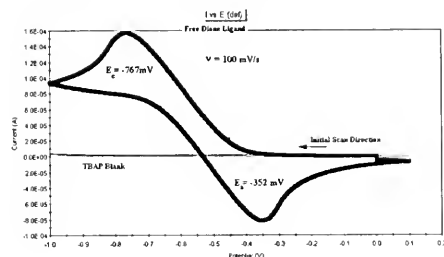


Figure 6. Cyclic Voltammogram of 1,10-phenanthroline-5,6-dione (dione). Acetonitrile solution of 0.03M dione and 0.20 M TBAP.

occurring at $E_{1/2} = 560$ mV and a peak-to-peak separation of 415 mV.

NMR

As expected, the ^1H -NMR showed three distinct proton environments for $[\text{Pt}(\text{dione})\text{Cl}_4]$, a doublet at $\delta(9.60)$, a doublet at $\delta(8.97)$, and a triplet at $\delta(8.33)$. These three proton signals integrated to 1:1:1.

Cytotoxicity Studies

Platinum compounds such as *cis*-platin and oxaliplatin have demonstrated anticancer activity. These compounds, like other anticancer agents, have serious side effects, due to the damage they cause to mitotically active cells. We thought it possible that $[\text{Pt}(\text{dione})\text{Cl}_4]$ might also have some anticancer activity. Therefore, cytotoxicity studies were undertaken to investigate 1) the potential chemotherapeutic utility of $[\text{Pt}(\text{dione})\text{Cl}_4]$, and 2) the effects of $[\text{Pt}(\text{dione})\text{Cl}_4]$ on rapidly dividing normal cells. The first study we report involved the cell lines G-401 and WI-38. The transformed cell line G-401 was derived from a rhabdoid tumor of the kidney of a 3 month old Caucasian male (68). The WI-38 cells are normal embryonic lung fibroblasts derived from a Caucasian female of 3 months gestation (69). As shown in Figure 7, panel A, only 37.9 % of the G-401 cells survived after 48 hours in 10 mM $[\text{Pt}(\text{dione})\text{Cl}_4]$, while 95.1 % of the WI-38 cells survived. This striking (2.5-fold) difference in survival rates was reproduced in five replicates and suggested that $[\text{Pt}(\text{dione})\text{Cl}_4]$ was selectively toxic to the malignant cells. Should $[\text{Pt}(\text{dione})\text{Cl}_4]$ progress to clinical trials, this selective toxicity might presage reduced toxicity to the normal cells of the patient.

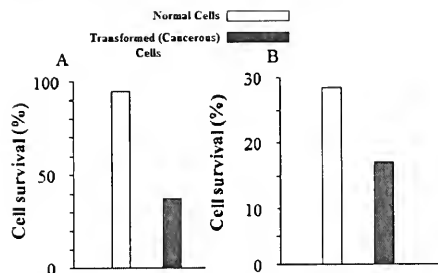


Figure 7. Response of normal and transformed cell lines to [Pt(dione)Cl₄]. Panel A shows the percent survival of the normal human cell line WI-38 and the transformed line G-401. Panel B shows the percent survival of the normal cell line Hs578Bst and the transformed line Hs578T. In both cases, the cells were exposed to 10 mM [Pt(dione)Cl₄] for 48 hours. Again we see a notable selectivity. We are currently screening a panel of 16 different cell lines. Results of that study will appear in a subsequent publication.

However, as WI-38 and G-401 were taken from different tissues of different individuals who were of different genders, the perceived selectivity might be due to differences in gene expression or individual biochemistry. In order to probe the cytotoxicity difference further, we tested [Pt(dione)Cl₄] against a matched pair of normal and transformed cell lines taken from a breast biopsy of a 74 year old Caucasian woman (70). The normal cell line, designated Hs578Bst, was derived from normal tissue adjacent to the tumor, and the transformed cell line, designated Hs 578T, was derived from the tumor itself. As is shown in Figure 7, panel B, in this case, 17.2 % of the breast cancer cells survived compared to 28.1 % of the normal breast cells, which represents a 1.6-fold difference. As the two cell lines were taken from the same individual, it appears that [Pt(dione)Cl₄] is demonstrating selective toxicity toward the malignant cells

DNA Binding Studies:

Based upon cell culture studies of tetraplatin, it is likely that [Pt(dione)Cl₄] is reduced to [Pt(dione)Cl₂] *in situ* (58;59). Looking at the structure of [Pt(dione)Cl₂] (See Figure 1) it is easy to imagine that [Pt(dione)Cl₂] might interact with DNA in a manner similar to that of *cis*-platin. It is well known that *cis*-platin derives its cytotoxicity from its preferential intrastrand binding of the N7 atoms of the imidazole rings of guanine {1,2-d(GpG) 60-65%} and adenine {1,2-d(ApG) 20-25%} (58;59).

We directly compared the electrophoretic migration rates of poly(dG-dG)-poly(dC-dC), poly(dG-dC)-poly(dG-dC), and poly(dA-dT)-poly(dA-dT) in the absence of any drug and then in the presence of [Pt(dione)Cl₄] and again with *cis*-platin. Figures 8 and 9 summarize the results of these experiments.

As expected, *cis*-platin had little effect on the migration rates of poly(dG-dC)-poly(dG-dC) (59;60) and likewise, [Pt(dione)Cl₄] had little effect on the migration rate of this same DNA strand. This suggests that in a manner similar to *cis*-platin, [Pt(dione)Cl₄] has little affinity for binding to adjacent guanines on opposite strands (interstrand) (59;60). We also noted that both *cis*-platin and [Pt(dione)Cl₄] had a very similar affinity for poly(dA-dT)-poly(dA-dT). The surprise was in the strong effect relative to *cis*-platin that [Pt(dione)Cl₄] had on poly(dG-dG)-poly(dC-dC). It has long been known that *cis*-platin derives its bioactivity from its strong binding affinity for bonding to adjacent guanines on the same strand (intrastrand). In our study, [Pt(dione)Cl₄] had an effect on poly(dG-dG)-poly(dC-dC) that was nearly five times more pronounced than what we saw for *cis*-platin. Even if the binding affinity of [Pt(dione)Cl₄] to poly(dG-

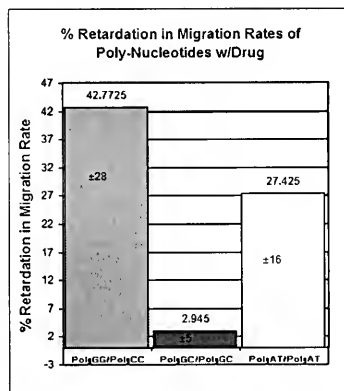


Figure 8. A comparison of the electrophoretic migration rates of poly(dG-dG)-poly(dC-dC), (Blue); poly(dG-dC)-poly(dG-dC) (Red), and poly(dA-dT)-poly(dA-dT) (Beige) Duplex DNA in the absence of [Pt(dione)Cl₄] vs gels containing 10 mM [Pt(dione)Cl₄]. Data is reported as a % reduction in the migration rate. Data is an average of four replicates and the standard deviation is shown in each bar.

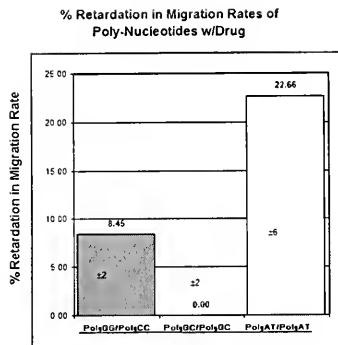


Figure 9. A comparison of the electrophoretic migration rates of poly(dG-dG)-poly(dC-dC) (Blue); poly(dG-dC)-poly(dG-dC) (average zero change), and poly(dA-dT)-poly(dA-dT) (Beige) Duplex DNA in the absence of cis-platin vs gels containing 10 mM cis-platin. Data is reported as a % reduction in the migration rate. Data is an average of three replicates and the standard deviation is shown in each bar.

dG)-poly(dC-dC) is much greater than that of cis-platin, nearly 65% of bound cis-platin is intrastrand linking to two adjacent guanines (58;59). It would be hard to account for such a dramatic difference in the observed affect if it were only due to a greater binding affinity of [Pt(dione)Cl₄] for poly(dG-dG)-poly(dC-dC).

Many quinones have been studied as anti-tumor agents (57). We speculate that [Pt(dione)Cl₄] may first bind to DNA through intrastrand binding to two adjacent guanines in a manner similar to that of cis-platin and then the quinone-dione interacts further with the DNA strand. We are planning a series of experiments that will compare the effects of cis-platin, [Pt(dipy)Cl₂] & [Pt(dione)Cl₂] on the electrophoretic migration rates of poly(dG-dG)-poly(dC-dC) and other select DNA duplexes. This will allow us to better understand the effect the dione moiety has on the observed change in the electrophoretic migration rates of these DNA duplexes.

Acknowledgments

Funding for this project was obtained through a generous grant from Sweet Briar College Faculty Grants, Sweet Briar College Summer Honors

Research Grant; The Jeffress Memorial Trust Grant # J490, and a Virginia Commonwealth Health Research Board Grant.

References

- (1). Photochemistry of [Ru(N-N)₂]²⁺.
(a) T.J. Meyer. *Prog. Inorg. Chem.*, **1983**, 30, 389.
(b) R.J. Watts. *J. Chem. Educ.*, **1983**, 60, 834.
3b Contains 90 cited references.
(c) N. Sutin.; C. Creutz. *J. Chem. Educ.*, **1983**, 60, 809-813.
- (2). A.E. Friedman, J.C. Chambron, J.P. Savvage, N.J. Turro; J.K. Barton. *J. Am. Chem. Soc.*, **1990**, 112, 4960—4962.
- (3). I. Hag, P. Lincoln, D. Suh, B. Norden, B.Z. Chowdhry; J.B. Chaires. *J. Am. Chem. Soc.*, **1995**, 117, 4788-4796.
- (4). S. Satyanarayana, J.C. Dabrowiak; J.B. Chaires. *Biochemistry*, **1992**, 31, 9319-9324.
- (5). J.K. Barton. *Pure and Appl. Chem.*, **1989**, 61, 563-564.
- (6). J.K. Barton. *Science*, **1986**, 233, 727-734.
- (7). J.K. Barton, J.J. Dannenberg; A. L. Raphael. *J. Am. Chem. Soc.*, **1982**, 104, 4967-4969.
- (8). J.K. Barton; A.L. Raphael. *Proc. Natl. Acad. Sci. USA*, **1985**, 82, 6460-6464.
- (9). J.K. Barton; A.L. Raphael. *J. Am. Chem. Soc.*, **1984**, 106, 2466-2468.
- (10). J.K. Barton, A.T. Danishefsky; J.M. Goldberg. *J. Am. Chem. Soc.*, **1984**, 106, 2172-2176.
- (11). J.M. Barton, J.M. Goldbert, J.M. Kumar; N.J. Turro. *J. Am. Chem. Soc.*, **1986**, 108, 2081-2088.
- (12). B.M. Goldstein, J.K. Barton; H.M. Berman. *Inorg. Chem.*, **1986**, 25, 842-847.
- (13). L.E. Pope; D.S. Sigman. *Proc. Natl. Acad. Sci. USA*, **1984**, 81, 3-7.
- (14). L.E. Marshall, D.R. Graham, K.A. Reich; D.S. Sigman. *Biochemistry*, **1981**, 20, 244-250.
- (15). D.S. Sigman. *Acc. Chem. Res.*, **1986**, 19, 180-186.
- (16). D.S. Sigman. In *Metal-DNA Chemistry*; ACS Symposium Series, 402; American Chemical Society, Washington D.C. (1989).
- (17). D.S. Sigman. "Chemical Nucleases." Lecture at Purdue University, **1990**.
- (18). D.P. Mack; P.B. Dervan. *J. Am. Chem. Soc.*, **1990**, 112, 4604-4606.
- (19). R.P. Hertzbert; P.B. Dervan. *J. Am. Chem. Soc.*, **1982**, 104, 313-315.
- (20). M.B. Fleisher, K.C. Waterman, N.J. Turro; J.K. Barton. *Inorg. Chem.*, **1986**, 25, 3549-3551.
- (21). A.M. Pyle, E.C. Long; J.K. Barton. *J. Am. Chem. Soc.*, **1989**, 111, 4520-4522.
- (22). H.Y. Mei; J.K. Barton. *J. Am. Chem. Soc.*, **1986**, 108, 7414-7416.

- (23) H.Y. Mei; J.K. Barton. *Proc. Natl. Acad. Sci. USA*, **1988**, 85, 1339-1343.
- (24) C.V. Kumar, J.K. Barton; N.J. Turro. *J. Am. Chem. Soc.*, **1985**, 107, 5518-5523.
- (25) J.P. Rehmann; J.K. Barton. *Biochemistry*, **1990**, 29, 1701-1709.
- (26) A. Sitlani, C.M. Dupureur; J.K. Barton. *J. Am. Chem. Soc.*, **1993**, 115, 12589-12590.
- (27) C.S. Chow; J.K. Barton. *J. Am. Chem. Soc.*, **1990**, 112, 2839-2841.
- (28) A.H. Krotz, B.P. Hudson; J.K. Barton. *J. Am. Chem. Soc.*, **1993**, 115, 12577-12578.
- (29) D. Suh; J.B. Chaires. *Bioorg. & Med. Chem.*, **1995**, 3, 6, 723-728.
- (30) S. Satyanarayana, J.C. Dabrowiak; J.B. Chaires. *Biochemistry*, **1993**, 2573-2584.
- (31) T. Yamamoto, Y. Saitoh, K. Anzai, H. Fukumoto, T. Yasuda, Y. Fujiwara, B. Choi, K. Kubota; T. Miyamae. *Macromolecules*, **2003**, 36, 6722-6729.
- (32) C.A. Goss; H.D. Abruña. *Inorg. Chem.*, **1985**, 24, 4263-4267.
- (33) Q. Wu, M. Maskus, F. Pariente, F. Tobalina, V.M. Fernandez, E. Lorenzo; H.D. Abruña. *Anal. Chem.*, **1996**, 68, 3688-3696.
- (34) F.M. MacDonnell; S. Bodige. *Inorg. Chem.*, **1996**, 35, 5758-5759.
- (35) Y. Lei; F.C. Anson. *J. Am. Chem. Soc.*, **1995**, 117, 9849-9854.
- (36) P.W. Paw; R. Eisenberg. *Inorg. Chem.*, **1997**, 36, 2287-2293.
- (37) A.Y. Girgis, Y.S. Sohn; A.L. Balch. *Inorg. Chem.*, **1991**, 30, 2895-2899.
- (38) Y. Lei, C. Shi; F.C. Anson. *Inorg. Chem.*, **1996**, 35, 3044-3049.
- (39) M. Yamadam, Y. Tanaka; Y. Yoshimoto; S. Kuroda; I. Smimao. *Bull. Chem. Soc. Japan*, **1992**, 65, 1006-1011.
- (40) G.A. Fox, S. Bhattachary; C.G. Pierpont. *Inorg. Chem.*, **1991**, 30, 2895-2899.
- (41) P.A. Bryngelson, T.S. Haddad; N.M. Doherty. *Abstracts of Papers*, 211th National Meeting of the American Chemical Society, New Orleans, LA, Spring 1996; American Chemical Society: Washington DC, 1996; INOR 38.
- (42) M. Shi; F.C. Anson. *Anal. Chem.*, **1998**, 70, 1489-1495.
- (43) T.S. Eckert; T.C. Bruice. *J. Am. Chem. Soc.*, **1983**, 105, 4431.
- (44) T.S. Eckert, T.C. Bruice; J.A. Gainor; S.M. Weinred. *Proc. Natl. Acad. Sci. USA*, **1982**, 79, 2553.
- (45) G. Hilt; E. Steckhan. *J. Am. Chem. Soc., Chem. Commun.*, **1993**, 1706.
- (46) S. Itoh, H. Fukushima, M. Komatsu; Y. Ohshiro. *Chem. Lett.*, **1992**, 1583.
- (47) R.D. Gillard; R.E.E. Hill. *J. Am. Chem. Soc., Dalton Trans.*, **1974**, 1217.
- (48) (a) D.H. Evans; D.A. Griffith. *J. Electroanal. Chem. Interfacial. Electrochem.*, **1982**, 134, 301 (b) *Ibid.* **1982**, 136, 149.
- (49) B. Spingler, D. Wittington; S. Lippard. *Inorg. Chem.*, **2001**, 40, 5596-5602.
- (50) S. Berger, J. Fiedler, R. Reinhardt; W. Kaim. *Inorg. Chem.*, **2003**, 43, 1530-1538.
- (51) J.G. Collins, A.D. Sleeman, J.R. Aldrich-Wright; I. Greguric; T.W. Hambley. *Inorg. Chem.*, **1998**, 37, 3133-3141.
- (52) R.M. Hartshorn; J.K. Barton. *J. Am. Chem. Soc.*, **1992**, 114, 5919-5925.
- (53) R.E. Holmlin, J.A. Yao; J.K. Barton. *Inorg. Chem.*, **1999**, 38, 174-189.
- (54) R.E. Holmlin, E.D.A. Stemp; J.K. Barton. *J. Am. Chem. Soc.*, **1996**, 118, 5236-5244.
- (55) K.E. Erkkila, D.T. Odom; J.K. Barton. *Chem. Rev.*, **1999**, 99, 2777-2795.
- (56) C.M. Dupureur; J.K. Barton. *Inorg. Chem.*, **1997**, 36, 33-43.
- (57) S.E. Wolkenberg; D.L. Boger. *Chem Rev.*, **102**(7) **2002**, 2477-2495.
- (58) M.A. Fuertes, C. Alonso; J.M. Perez. *Chem Rev.*, **2003**, 103, No.3.
- (59) (a) E. Wong; C.M. Giandomenico. *Chem. Rev.*, **1999**, 99, 2451-2466. (b) E.R. Jamieson; S.J. Lippard *Chem Rev.*, **1999**, 99, 2467-2498.
- (60) Full System Reference : E.J. Gabe, Y. Le Page, J.P. Charland, F.L. Lee; P.S. White. *J. Appl. Cryst.*, **1989**, 22, 384-387.
- (61) Scattering Factors from *Int. Tab. Vol. 4: International Tables for X-ray Crystallography, Vol. IV*, Kynoch Press, Birmingham, England (1974).
- (62) ORTEP Plotting: C.K. Johnson. *ORTEP - A Fortran Thermal Ellipsoid Plot Program, Technical Report ORNL-5138*, Oak Ridge (1976).
- (63) W.B. Connick, L.M. Henling, R.E. Marsh; H.B. Gray. *Inorg. Chem.*, **1996**, 35, 6261-6265.
- (64) K.N. Crowder, S.J. Garcia, R.L. Burr, J.M. North, M.H. Wilson, B.L. Conley, P.E. Fanwick, P.S. White; K.D. Sienerth; R.M. Granger, II. *Inorg. Chem.*, **2004**, 43 (1), 72-78.
- (65) R. Granger, J.N. Granger, K.D. Sienerth, J.M. North, M.H. Wilson, T.H. Luong, S.J. Garcia; K. del Campo. *J. Und. Chem. Res.*, **2002** 3, 95.
- (66) R.M. Granger, II, J.N. Granger, P.E. Fanwick, K. del Campo; M.B. Becherer. *Virginia Academy of Science*, **1999**, 50(1), 7.
- (67) N. Walker; D. Stuart. *Acta Crystallogr.*, **1983**, A39, 158.
- (68) A.J. Garvin, G.G. Re; B.I. Tarnowski, D.J. Hazen-Martin; D.A. Sens. The G401 cell line, utilized for studies of chromosomal changes in Wilms' tumor, is derived from a rhabdoid tumor of the kidney. *Am. J. Pathol.*, **1993**, 142: 375-380.

- (69). L. Hayflick and P.S. Moorhead. The serial cultivation of human diploid cell strains. *Exp. Cell Res.*, **1961**, 25: 585-621.
- (70). A.J. Hackett, H.S. Smith, E.L. Springer, R.B. Owens, W.A. Nelson-Rees, J.L. Riggs; M.B. Gardner. Two syngenic cell lines from human breast tissue: the aneuploid mammary epithelial (Hs 578T) and the diploid myoepithelial (Hs 578Bst) cell lines. *J. Natl. Cancer Inst.*, **1977**, 58: 1795-1806.

LIST OF FIGURES

	<u>Page</u>
Figure 1: X-ray crystal structure of $[\text{Pt}(\text{dpk})\text{Cl}_4]$, anhydrous and hydrated form.....	2
Figure 2: Vials containing $[\text{Pt}(\text{dpk})\text{Cl}_4]$ at the time of purging with CO_2 and after 48 h.....	3
Figure 3: Bioanalytical Systems bulk electrolysis cell model # MF-1056.....	11
Figure 4: Cyclic Voltammogram from a solution of $[\text{Pt}(\text{dpk})\text{Cl}_4]$ in acetonitrile.....	14
Figure 5: Cyclic Voltammogram showing the electrocatalytic reduction of CO_2	15
Figure 6: GC/MS-1 and GC/MS-2.....	16
Figure 7: NMR-1.....	17
Figure 8: X-ray crystal structure of the hydrated form of $\text{Pt}(\text{dpk})_2\text{Cl}_2[\text{PF}_6]$	18
Figure 9: FT-IR Spectrum of $\text{Pt}(\text{dpk})_2\text{Cl}_2[\text{PF}_6]$	18
Figure 10: GC/MS of diethyl oxalate from catalytic reduction of CO_2	19
Figure 11: GC/MS of commercially obtained diethyl oxalate.....	19
Figure 12: GC/MS of various organic molecules from catalytic reduction of CO_2	20
Figure 13: ^{13}C -NMR of the product from our $^{13}\text{CO}_2$ run.....	21
Figure 14: X-ray crystal structure of our Polymer-dpk catalyst.....	22
Figure 15: NMR-2 and NMR-3.....	23
Figure 16: NMR-4.....	24

LIST OF SCHEMES

	<u>Page</u>
Scheme 1: Proposed mechanism for the hydration of $[\text{Pt}(\text{dpk})\text{Cl}_4]$	3
Scheme 2: Addition of CO_2^- radical anions to cyclohexene.....	4
Scheme 3: Two possible CO_2 reduction pathways.....	5
Scheme 4: Diagram of C. Kubiak's catalytic dimer for the reduction of CO_2 to oxalate.....	6
Scheme 5: The proposed mechanism of the $[\text{Pt}(\text{dpk})_2\text{Cl}_2]^{2+}$ reduction catalyst.....	7
Scheme 6: Electrocatalytic reduction of CO_2 at the surface of the electrode.....	15

How to utilize CO₂? Studies of a Novel CO₂ Reduction Catalyst

SECTION 1: INTRODUCTION

Section 1.1: Why CO₂?

Carbon dioxide is the end product of many industrial and biological processes; however, only plants, algae, and certain bacteria can effectively regenerate useful organic products from this abundant molecule.² Activation of CO₂ by bioconversion, thermal heterogeneous and homogeneous reduction, photochemical reduction, and coordination to transition metals² experiments have all been investigated. Specific interest has developed in redox mediators that are able to catalyze the electrochemical reduction of CO₂ accompanied by carbon-carbon bond formation, thus mimicking photosynthesis.^{1,3-12} Photosynthesis converts CO₂ to organic material by reducing CO₂ to carbohydrates in a rather complex set of reactions. Electrons for this reduction ultimately come from water, which is then converted to oxygen and protons. Energy for this process is provided by light. In plants, the enzyme's active site consists of an iron-sulfur complex,¹³ which initiates reduction of CO₂ upon absorption of a photon by chlorophyll. The structure of the enzyme's active site has been determined, yet the enzyme's activity outside of living tissue has not been duplicated to date. Therefore, understanding of the process of CO₂ reduction, by trying to mimic it, is of fundamental importance.

There is an economic incentive for developing CO₂ reduction catalysts for applications in closed environments, such as submarines and space stations, which would improve the current technology used for the clean up of aerobic by-product (CO₂). Current "scrubbers" simply trap the CO₂ and must be replaced or recharged upon saturation. An ideal system would *both* remove CO₂ continuously and produce useful organic molecules (carbon-carbon bonds), in effect a compact "artificial photosynthetic" device. A novel catalytic system that will selectively produce carbon-carbon bonds from CO₂ and that will ultimately lead to the development of such an "artificial photosynthetic" device is the focus of this research.

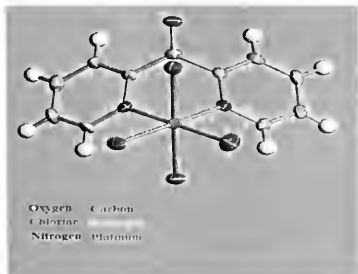
Section 1.2: Activation of CO₂ and Carbon-Carbon Bond Formation

The reduction of CO₂ is the first step in the formation of carbon-carbon bonds using CO₂ as a feed stock.¹ The electrochemical reduction of CO₂ by transition metal catalysts has acquired much attention over the past two decades.^{1,3-12}

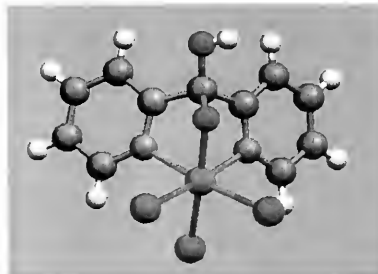
Investigation into the properties of the ligand di-2-pyridyl ketone (dpk) was first reported in 1967 by R. R. Osborne and W. R. McWhinnie.¹⁴ Their work focused on the co-ordination of dpk in copper(II) halide and perchlorate complexes. In the time since this first study, metal ion complexes with dpk have been reported for Nickel(II),¹⁵⁻²³ Iron(II) and Iron(III),^{15,17,19} Manganese(II),^{15,21} Uranium(VI),²³ Cobalt(II) and Cobalt(III),^{15,17,19,21,24} Zinc(II),^{15,21,23,25} Cadmium(II),²⁵ Mercury(II),²⁵ Copper (I) and Copper(II),^{15,21-23,26-31} Chromium(III),²⁷ Ruthenium(II),^{27,32} Rhenium(I) and Rhenium(V),^{33,34} Silver(I),³⁵ Antimony(III),³⁶ Palladium(II),³⁷ Gold(III),³⁷ and Platinum(II).^{37,38} To date, there has been only two studies on M(IV) dpk complexes, ours³⁹ and one which focused on Tin(IV).⁴⁰

After the initial coordination with the metal ion, the dpk ligand is subject to nucleophilic attack by water in the presence of many different metal ions, including but not limited to Ni(II), Co(III), Cu(II), Cr(III), Sb(III), Pd(II), Au(III), and Pt(II).³⁵ In December of 2003, we reported on the synthesis of a platinum(IV) compound containing a di-2-pyridyl (dpk) ligand that is stable both in its anhydrous form [Pt(dpk)Cl₄] (**1a**) (Figure 1), and in its hydrated form [Pt(dpk-O-OH)Cl₃] \cdot HCl (**1b**) (Figure 1).³⁹ The literature reveals that many complexes produced analogous compounds by activation of small alcohols such as methanol or ethanol. For this reason, our group decided to explore the possibility of activating carbon dioxide with our tetrachloro(di-2-pyridyl ketone) platinum(IV), [Pt(dpk)Cl₄], catalyst.

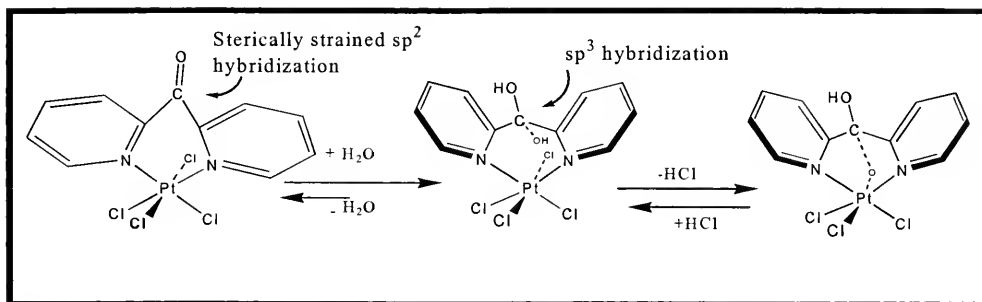
Figure 1. A) [Pt(dpk)Cl₄] **1a**



B) hydrated form of [Pt(dpk)Cl₄] **1b**



The crystal structure of the hydrated form shows that one of the hydroxyl groups from the resulting *gem*-diol has undergone a cyclometallation/condensation reaction resulting in an oxygen atom directly coordinated to the Pt(IV) center and the ejection of an HCl molecule (Scheme 1).³⁹



Scheme 1. Proposed mechanism for the hydration of Pt(dpk)Cl₄

We also explored the addition of other small molecules across the dpk ketone.⁴¹ A stream of CO, CO₂ and H₂ gases was bubbled through vials containing our [Pt(dpk)Cl₄] catalyst dissolved in acetonitrile. The addition of gases resulted in a dramatic color change in each vial, which was a suggestive evidence of the addition of these gases across the dpk ketone. Figure 2 shows a the three vials both at the time of initial purging (A) and after 48 hours in contact with the gasses (B).

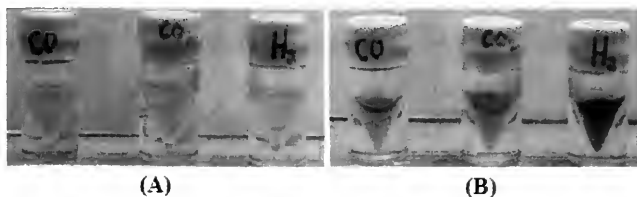
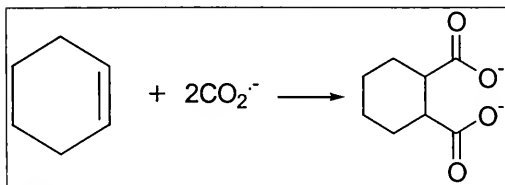


Figure 2: (A) Time = 0 h of a 3.0 mM solution of **1** in acetonitrile purged with CO, CO₂ or H₂ respectively: (B) Time = 48 h of a 3.0 mM solution of **1** in acetonitrile purged with CO, CO₂ or H₂ respectively.

After 48 h the septa were removed. When the mechanical pressure was exerted on the green paste during the preparation of the IR pellet, the colors of the paste reverted to the original colors (A). This implies that CO, CO₂ and H₂ activated **1** and the process is reversible. FT-IR also confirms the regeneration of the catalyst upon the removal of the substrates.⁴¹

Next we wanted to demonstrate the electrochemical reduction of CO₂, using [Pt(dpk)Cl₄] catalyst, by observing an increased current in the reduction wave in the presence of CO₂. These experiments were conducted in collaboration with a research group at Elon University.

The most recent research has focused on exploring the possibility of reducing CO₂ with our **1** catalyst and trapping CO₂^{•-} radical anions with cyclohexene.⁴² Initial bulk electrolysis experiments were done hoping to obtain cyclohexanedicarboxylate (Scheme 2).



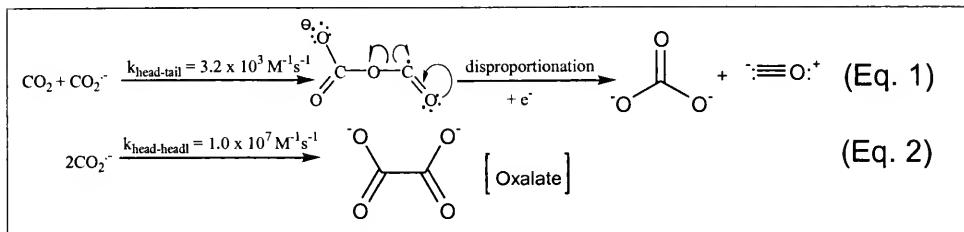
Scheme 2. Addition of CO₂^{•-} radical anions to cyclohexene

When a CO₂ molecule becomes reduced it becomes a free radical anion, CO₂^{•-}. These radical anions react with the first molecule they come in contact with. When two CO₂^{•-} radicals “bump” into each other, they can share two electrons to form a carbon-carbon bond. The simplest carbon-carbon bond containing compound derived from CO₂ is oxalate. In nature, the process of photosynthesis uses two electrons and two molecules of carbon dioxide simultaneously. The homogenous electrocatalysts for the reduction of CO₂ that are reported in the literature usually catalyze the CO₂ reduction to either formate or CO together with H₂ formation,^{5,6,12} oxalate,⁸ methane,⁵ glycolate and glyoxylate,⁴³ formic acid and formaldehyde.⁴⁴

A difficult challenge in obtaining oxalate is overcoming the disproportionation of the single-electron transfer product, CO₂^{•-} to CO and CO₃²⁻ (Scheme 3, Equation 1). Even though the kinetics of the dimerization reaction leading to the formation of oxalate (Scheme 3, Equation 2)

are much faster, the disproportionation reaction predominates due to a very low concentration of $\text{CO}_2^{\cdot -}$ compared to the concentration of CO_2 molecules. Hence, the goal is to manipulate the chemical environment so that two $\text{CO}_2^{\cdot -}$ can react with each other before reacting with CO_2 molecules.

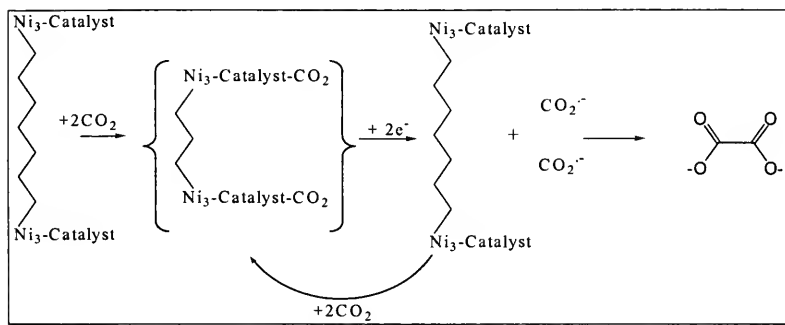
Scheme 3. Two Possible CO_2 Reduction Pathways



Section 1.3: Synthesis of a Carbon-Carbon Bond Forming CO₂ Reduction Catalyst

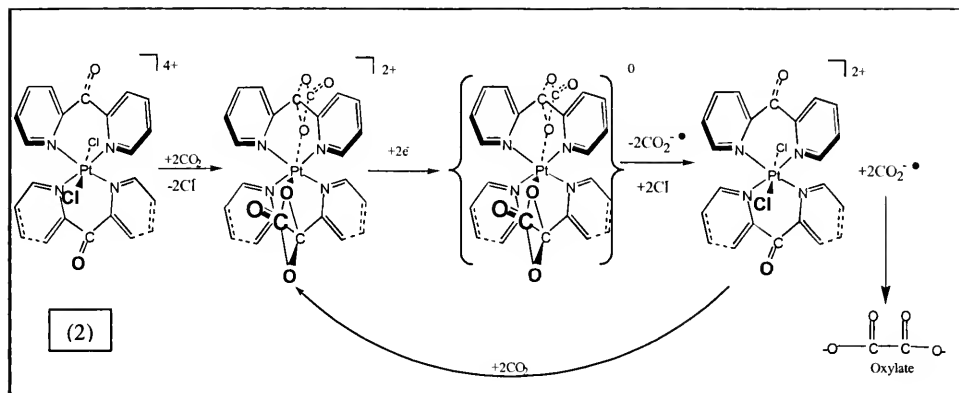
One research group has worked with a nickel-based catalyst and reported the formation of oxalate.^{42,45} Their work was focused on the synthesis of a catalyst that has two catalytic centers in close proximity to each other (Scheme 4).⁴² The group successfully isolated several micrograms of oxalate.

Scheme 4. Diagram of C. Kubiak's catalytic dimer for the reduction of CO₂ to oxalate



Based on these results, our research began focusing on designing a catalytic system that would have two catalytic sites on the same metal, so that two CO₂ molecules could simultaneously be reduced in close proximity to each other (Scheme 5). The platinum family (Ni, Pd, and Pt) is capable of a 2-electron transfer due to its preference to change oxidation states two electrons at a time {Pt(IV) → Pt(II) → Pt(0)}. This characteristic of platinum facilitates the simultaneous production of two CO₂⁻ radicals needed for carbon-carbon bond formation (Scheme 3).

Scheme 5. The proposed mechanism of the $[\text{Pt}(\text{dpk})_2\text{Cl}_2]^{2+}$ reduction catalyst



Prior research in this group had demonstrated that CO₂ would reversibly bind to the Pt(dpk) moiety and had suggested CO₂ activation. However, full characterization of $[\text{Pt}(\text{dpk})_2\text{Cl}_2]^{2+}$ (2) and its catalytic potential had not been fully explored.

SECTION 2: PROJECT OBJECTIVES

The main focus of this research can be broken down into the following research goals:

1. Completion of the study of electrocatalytic reduction of CO₂ using **1** as the catalyst.
2. Synthesis of the catalyst **2**.
3. Completion of the spectroscopic characterization of the catalyst **2**.
4. Understand the reaction conditions that result in CO₂ reduction with **2**.
5. Isolate and characterize the CO₂ reduction products formed and relate this to credible mechanisms.

In particular, this research has focused on the electrocatalytic reduction of CO₂ using compounds **1** and **2** and analysis of the CO₂ reduction products formed.

SECTION 3: CHEMICALS AND EQUIPMENT

Chemicals

The chemicals: di-2-pyridyl ketone (dpk), potassium hexachloroplatinate(IV) (K_2PtCl_6), iodoethane, potassium hexafluorophosphate (KPF_6), acetonitrile, and diethyl ether were purchased from Aldrich Chemical Company. Acetonitrile was distilled. Silver tartrate was made using 1:2 mole ratio of d-tartaric acid and silver nitrate, respectively; dissolved separately in distilled water, mixed together and precipitated with acetone.

Equipment

- Princeton Applied Research EG&G Model 263A potentiostat/galvanostat system.
- Working platinum mesh electrode, BAS.
- Counter electrode: coiled 23 cm platinum wire within a fritted glass isolation chamber, BAS part #MW-1033.
- RE-5B Ag/AgCl reference electrode, BAS part #MW-2052.
- Bone Dry Grade 2.8TM CO₂ Gas from Arcet Welding Supplies.
- Matteson Instruments 4020 Galaxy Series FT-IR.
- JEOL 400 MHz NMR Spectrometer.
- 5890 Series II Gas Chromatograph/5972 Series Mass Selective Detector.

SECTION 4: EXPERIMENTAL

Section 4.1: Synthesis of $[\text{Pt}(\text{dpk})_2\text{Cl}_2][\text{PF}_6]_2$

A sample of K_2PtCl_6 (0.1 g, 0.21 mmol) was dissolved in 25 mL of distilled water. A large molar excess of dpk relative to Pt (*ca.* 0.2 g) was dissolved in 5 mL of distilled water, added to the K_2PtCl_6 solution, and stirred for ~ 1 h. When a yellow precipitate formed, $\text{Ag}_2(\text{tart})$ (0.07 g, 0.21 mmol) was added and the solution was refluxed for 65 min, or until white precipitate of AgCl started forming. The solution was filtered through a sintered glass buchner funnel (frit) to remove AgCl , and a pale yellow filtrate remained. Excess dpk was added (*ca.* 0.2 g), and the solution was allowed to stir overnight. The solution was heated below the B.P. until it was hot. Excess KPF_6 was added. After heating, the solution was placed on ice for ~ 10 min. Once cool, the solution was filtered and white/pale yellow solid was collected on a sintered glass buchner funnel. The solid was recrystallized from acetone/ether, and dried *in vacuo* overnight.

Section 4.2: Crystal chamber set-up

A saturated solution of $[\text{Pt}(\text{dpk})_2\text{Cl}_2]^{2+}$ in acetone was set in a small test tube, which was placed in a round bottom flask with diethyl ether that was then closed and purged with CO_2 . The purging of the flask with CO_2 was done to potentially add CO_2 across the dpk ketone and obtain a crystal structure with CO_2 bound to the catalyst. The flask was left on a shelf for *ca.* 80 h. The next Monday crystals had formed, and one suitable was sent to Purdue University for an x-ray structure determination.

Section 4.3: Electrocatalytic reduction of $[\text{Pt}(\text{dpk})\text{Cl}_4]$

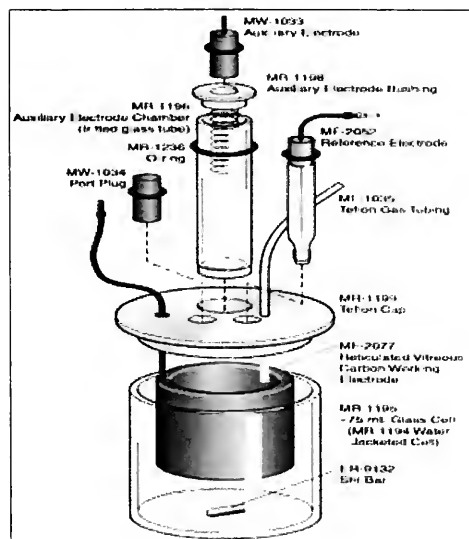
Solvents and glassware were dried and prepared as described previously:¹² before being placed in the drybox antechamber, all glassware was rinsed five times with DI water, rinsed with ethanol and air-dried. It was then dried at 220°C for >12 h before being transferred directly to the antechamber while still hot. All components of the electrochemical cell were rinsed with DI water and ethanol and dried *in vacuo* for >12 h at 75°C . The working electrode was either a 3 mm glassy carbon disk (BAS) or a 1 mm polished platinum disk (BAS). The counter electrode

was a platinum coil and the reference electrode was a silver wire immersed in a 0.01 M AgNO_3 solution in CH_3CN . The reference and counter electrodes were each separated from the bulk solution by a Vycor frit. In all electrochemical studies, the supporting electrolyte was 0.2 M tetrabutylammonium hexafluorophosphate (TBAP, Aldrich).

Section 4.4: Bulk Cell Electrolysis Experiments

Bulk electrolysis experiments were conducted using Bioanalytical Systems bulk electrolysis cell model number MF-1056 using platinum gauze as the working electrode, platinum as the counter electrode, and Ag/AgCl as the reference electrode. Figure 3 shows the bulk electrolysis cell model used for the CO_2 reduction experiments.

Figure 3. Bioanalytical Systems bulk electrolysis cell model # MF-1056



Bulk cell electrolysis of **2** was conducted in the presence of CO_2 in 0.2 M solution of KPF_6 in acetonitrile. The compound **2** was dissolved in ~ 50 mL of acetonitrile and purged for ~ 10 min. Afterward, at a potential of -1.5 V and current of 100 mA, the cell was turned on for *ca.* 15 min.

Bulk cell electrolysis experiments done with compound **1** were conducted in a similar way. The only differences are the potential (-2.0 V) and ~4.5 mL of cyclohexene was added to the acetonitrile solution.

Section 4.5: Product Extraction Procedure (1)

The majority of the electrolysis solution was removed by rotary evaporation. The resulting sludge was dissolved in ~25 mL of DMF. Several drops of iodoethane were added and the solution was allowed to stir overnight until it changed color to a bright yellow. The solution was extracted using ~20 mL of hexane (four times). The hexane layers were rinsed with ~25 mL of 2 M HCl to neutralize any remaining DMF, and then concentrated *in vacuo* to 5-10 mL, making it suitable for GC/MS analysis.

Product Extraction Procedure (2)

The bulk cell electrolysis solution was removed by rotary evaporation. A stir bar was placed in the flask, which was placed on a vacuum line overnight. The flask was purged with N₂ gas in the morning, then ~7 mL of iodoethane was added with a syringe and the solution was left to stir overnight. The next morning, ~11 mL of 0.1 M NaOH and ~10 mL of ethyl acetate was added to the flask containing iodoethane and left to stir for ~1 h. This solution was reduced down to ~1 mL using rotary evaporation. The remaining sludge was a yellow, thick liquid with some solid left in it. The sludge was dissolved in methanol resulting in “grease” forming on the surface of the solution. That solution was filtered through a Buchner funnel and then rinsed with ethylacetate. The ethyl acetate filtrate was reduced using rotary evaporation, and dried *in vacuo* for a week. Trace amounts were obtained and used for the analysis.

Product Extraction Procedure (3)

The volume of the electrolysis solution was reduced using rotary evaporation. The remaining white and yellow solid was dissolved in ~50 mL of Absolute ethanol and ~0.5 mL of iodoethane, then refluxed for 30 min. The solution color changed from pale yellow to dark yellow, and more white solid formed on the bottom of the flask (most likely KPF₆ or **1** since both are insoluble in ethanol).

Section 4.6: Esterification of a Commercially-Obtained *trans*-1,2-cyclohexanedicarboxylic acid

A sample of 0.05 g of *trans*-1,2-cyclohexanedicarboxylic acid was dissolved in ~100 mL of 200 Proof ethanol. The solution was refluxed for an hour, and then ~0.5 mL of iodoethane was added, and the solution was left to stir for 48 h.

Section 4.7: Esterification of a Commercially-Obtained Oxalic Acid

A sample of 0.11 g of oxalic acid was dissolved in 7.5 mL of iodoethane (1:93 mole ratio) and left to stir for *ca.* 120 h. About 11 mL of 0.1 M NaOH and 11 mL of ethyl acetate was added to the flask, when two layers formed, and it was refluxed for 1 h. The solution was worked up with 0.1 M NaOH and brine, and dried over MgSO₄. The ethyl acetate was removed by rotary evaporation and the remaining yellowish solid was dried *in vacuo* for a week.

Section 4.8: Synthesis of Poly-dpk Catalyst⁴⁶

A solution of K₂PtCl₄ was dissolved in distilled water and equimolar amount of Ag₃Citrate was added. A pinkish solution formed, and allowed to spin over night. The solution was refluxed (covered with aluminum foil) until the solution turned brown/black. The solution was then filtered through celite and a pale yellow filtrate was collected. The mole ratio of 2:1 of dpk to the metal was added to the pale yellow filtrate and allowed to spin until all dissolved. Then a 2:1 mole ratio of KPF₆ salt was added and a yellowish precipitate formed. This precipitate was filtered, dried *in vacuo* and recrystallized by dissolving it in acetone and precipitating it out with ether. A pale yellow precipitate was then collected on a frit and dried *in vacuo*.

SECTION 5: RESULTS AND DISCUSSION

Section 5.1: Electrocatalytic Reduction of [Pt(dpk)Cl₄]

Figure 4 shows a typical cyclic voltammogram obtained from a solution of Pt(dpk)Cl₄ in acetonitrile (work done in the Chemistry Department at Elon University, NC). The initial reduction (-0.5 V) is a 2-electron process which is most likely metal-centered, resulting in a Pt(II) complex, whereas the final reduction (-1.2 V) process involves the dpk ligand. The oxidation process observed at +0.75 V is related to the initial reduction, as demonstrated in Figure 5. Similarly, the oxidation observed at -1.1 V is the return wave for the final reduction wave.

If Pt(dpk)Cl₄ were to be involved in the heterogeneous catalytic reduction of CO₂, one would expect an increase in the reduction current associated with the disappearance of one of the oxidation waves.³⁹ Figure 5 demonstrates such behavior; furthermore, catalysis appears to occur at approximately -0.45V vs AgCl. This potential is nearly a full volt lower than those previously reported for other CO₂ reduction catalysts^{1,39-41} and nearly two volts lower than that of neat CO₂.³⁹

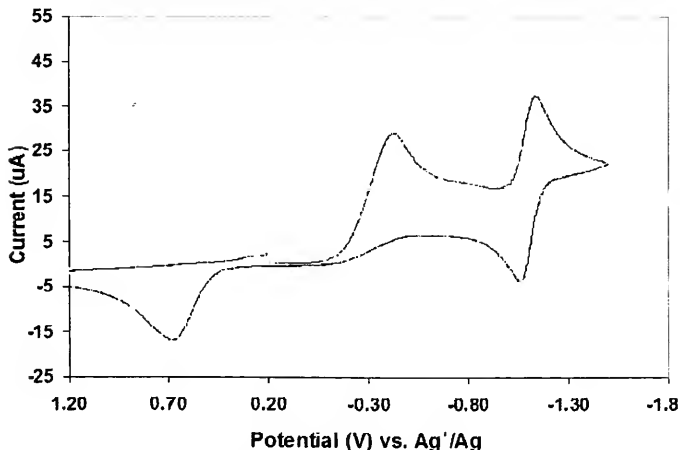


Figure 4. Cyclic voltammogram obtained from a 3.0 mM solution of **1** in CH₃CN. Working electrode: glassy carbon disk (3 mm diameter); Scan rate: 100 mV/s; 0.20 M TBAP.

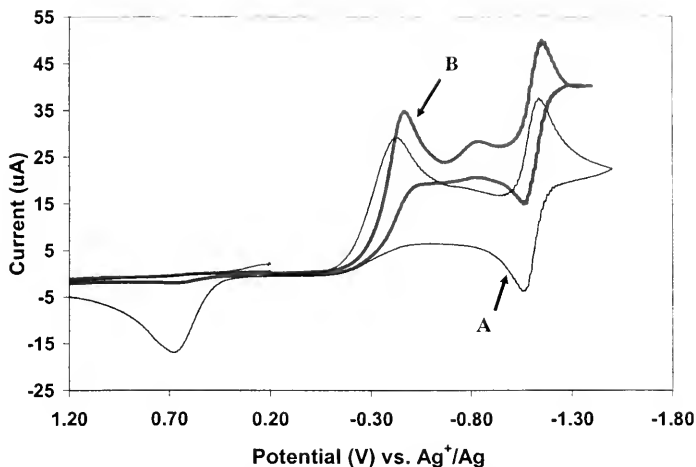
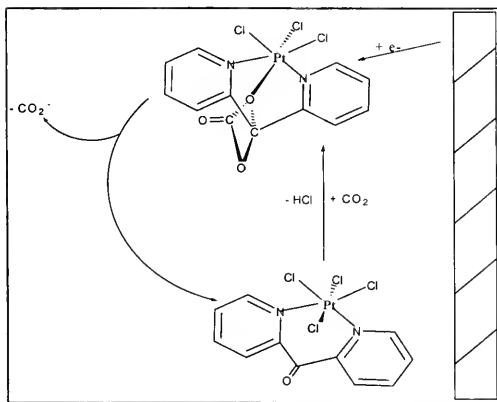


Figure 5. A. Cyclic voltammogram of a 3.0 mM solution of **1** in CH_3CN . Working electrode: Pt disk (1 mm diameter); scan rate: 100 mV/s; 0.20 M TBAP. B. Same solution as in A, after purging with anhydrous CO_2 for 10 min.

Scheme 6 shows the electrocatalytic reduction of CO_2 at an electrode's surface. When a CO_2 molecule is added across the dpk ketone, and the catalyst accepts an electron from the electrode and transfers it to the CO_2 molecule, the CO_2^- radical anion can then leave. This regenerates the reoxidized form of the catalyst, which is now ready to bind another CO_2 molecule, and the cycle repeats.

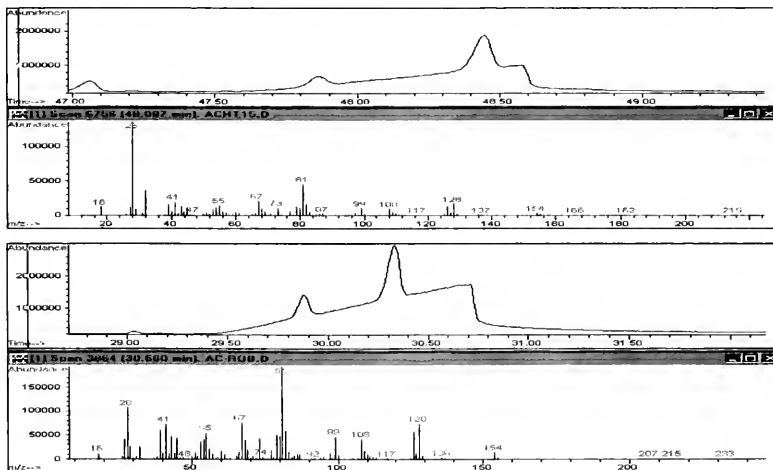


Scheme 6. Electrocatalytic reduction of CO_2 at the surface of the electrode

Recent experiments that focused on the possibility of reducing CO_2 with our 1 catalyst and trapping $\text{CO}_2^{\cdot-}$ radical anions with cyclohexene were first analyzed using GC/MS; these results strongly suggested the presence of the esterified cyclohexanedicarboxylic acid. However, the following NMR data did not agree with the GC/MS data. Since we had predicted that the electrolysis product would be cyclohexanedicarboxylic acid (or possibly a potassium salt), we had to run solubility tests and control experiments first. These constituted of finding the right method of esterifying a commercially obtained *trans*-1,2-cyclohexanedicarboxylic acid, so that it could be analyzed on the GC/MS.

When we compared the mass spectra of the esterified commercially-obtained cyclohexanedicarboxylic acid (see Sec 4.6) and of our esterified electrolysis product (see Product Extraction Procedure 3), they seemed identical (Figure 6). However, the ^1H -NMR of our product did not show the desired peaks, which we were not able to fully understand (Figure 7). ^1H -NMR of iodoethane and cyclohexene was also taken to make sure we had no contaminants coming from them (NMR-5 and NMR-6, respectively).

Figure 6. GC/MS1 and GC/MS-2



Section 5.2: Spectroscopic characterization of $[\text{Pt}(\text{dpk})_2\text{Cl}_2][\text{PF}_6]$

The structure of $[\text{Pt}(\text{dpk})_2\text{Cl}_2]^{2+}$ was confirmed by x-ray analysis. The structure is seen in Figure 8. All the crystallographic data are shown in Appendix A. Figure 9 presents the FT-IR spectrum of our $[\text{Pt}(\text{dpk})_2\text{Cl}_2]^{2+}$. The peak at 1700 cm^{-1} is the dpk ketone stretch. However, the IR spectrum shows an $-\text{OH}$ stretch *ca.* 3100 cm^{-1} , which indicated the mixture of both the anhydrous and the hydrated form of **2**.

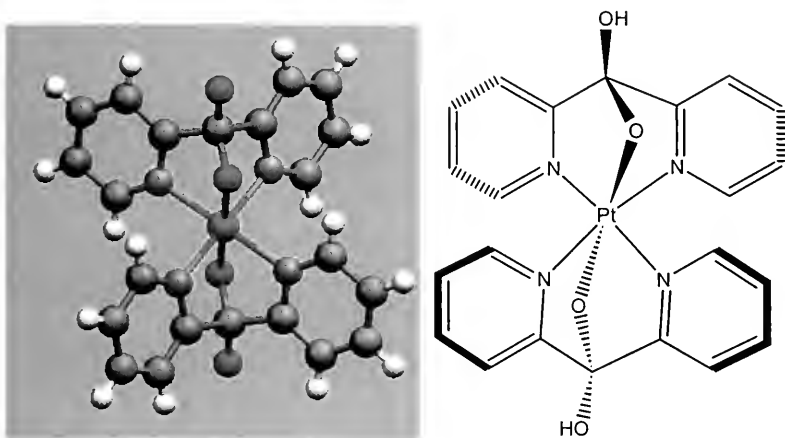


Figure 8. X-ray crystal structure of the hydrated form of $[\text{Pt}(\text{dpk})_2\text{Cl}_2][\text{PF}_6]$

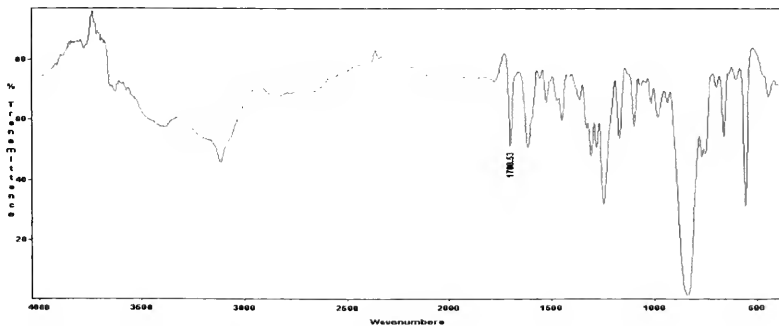


Figure 9. FT-IR spectrum of $[\text{Pt}(\text{dpk})_2\text{Cl}_2][\text{PF}_6]$

Section 5.3: Carbon-Carbon Bond Formation

After the initial synthesis of $[\text{Pt}(\text{dpk})_2\text{Cl}_2]^{2+}$ we ran experiments in our bulk cell hoping to obtain oxalate using $[\text{Pt}(\text{dpk})_2\text{Cl}_2]^{2+}$ catalyst. The electrolysis products were esterified (see Product Extraction Procedure (1) and analyzed using GC/MS. Figure 10 shows the mass spectrum of diethyloxalate from catalytic reduction of CO_2 and Figure 11 shows the MS of commercially obtained diethyloxalate. This was a suggestive evidence that we have successfully formed the simplest carbon-carbon bond.

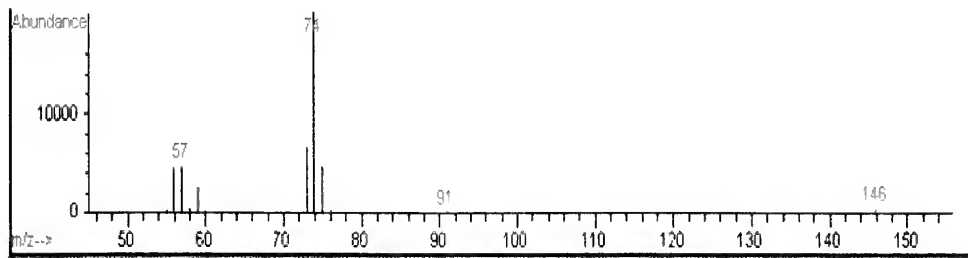


Figure 10. GC/MS of diethyl oxalate from catalytic reduction of CO_2

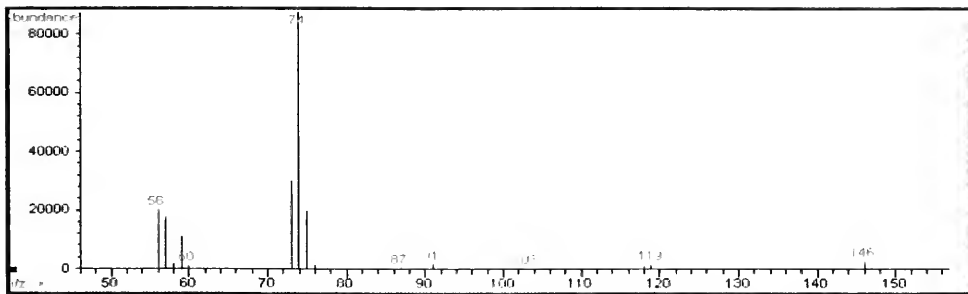


Figure 11. GC/MS of commercially obtained diethyloxalate

However, the next set of experiments, which we performed the next summer, followed the same procedure and appeared to have given different results; those did not include oxalate but more complex organic molecules (Figure 12).

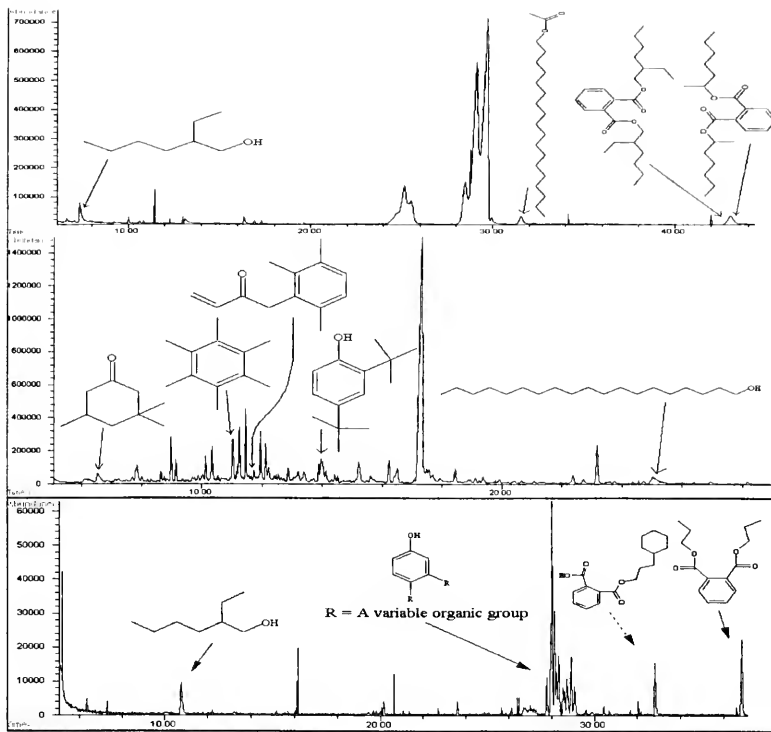


Figure 12. GC/MS of various complex organic molecules from catalytic reduction of CO₂

Since the percentage confidence was 98-99 %, we thought that these molecules, which are commonly found in plants, were contaminants in our reactor, such as plasticizers. We ran the following controls:

1. CO₂ bubbled through cell with no catalyst, no voltage applied.
2. CO₂ was bubbled through the cell, no catalyst present, a voltage of -1.7V was applied.
3. Cell with no catalyst, no CO₂ purge. Voltage of -1.7V applied.
4. Cell with catalyst present, voltage of -1.7V applied. Argon gas was bubbled through the cell in place of CO₂ using the same tubing as the CO₂.

All controls failed to reproduce the formation of organic molecules. Only when the catalyst was reduced in the presence of CO₂ did we find organic products in the reaction solution.

In order to be absolutely sure that the carbons were coming from CO₂ molecules, we decided to perform labeling study and use ¹³CO₂ instead of regular CO₂ gas. This experiment was conducted the same way as previously, except that the duration of the electrolysis run was *ca.* 3 min (versus 2-3 h). Figure 13 shows the ¹³C-NMR spectrum of our catalysis product. The peaks were obtained after only 5 min and the signals came off-scale compared to the solvent.

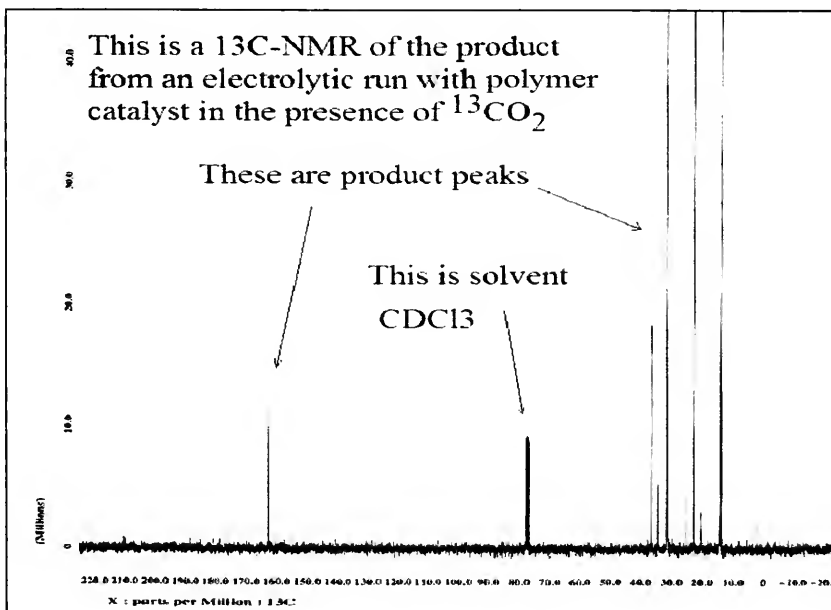


Figure 13. ¹³C-NMR of the product from our ¹³CO₂ run

Due to the organic molecules' complexity, we were not able to find a reasonable answer to how we managed to obtain these organic molecules. Therefore, we came to a conclusion that we must have made changes to our thought-to-be the catalyst **2**. Therefore, we went back to our notebooks and noticed a slight change in the synthesis of our [Pt(dpk)₂Cl₂]²⁺ catalyst.⁴⁶ In order to understand the changes that led to the formation of those organic molecules, we decided to

grow a crystal of what we thought might be a new catalyst we have developed by changing the procedure a little (see Section 4.5).⁴⁶ Figure 14 presents the crystal structure of our new polymer catalyst. It contains many dpk ligands on it and hence has many active sites where CO₂ molecules can be reduced. The crystal structure was a step forward to understanding the formation of complex molecules as a result of the formation of a high concentration of CO₂^{•-} radical anions.

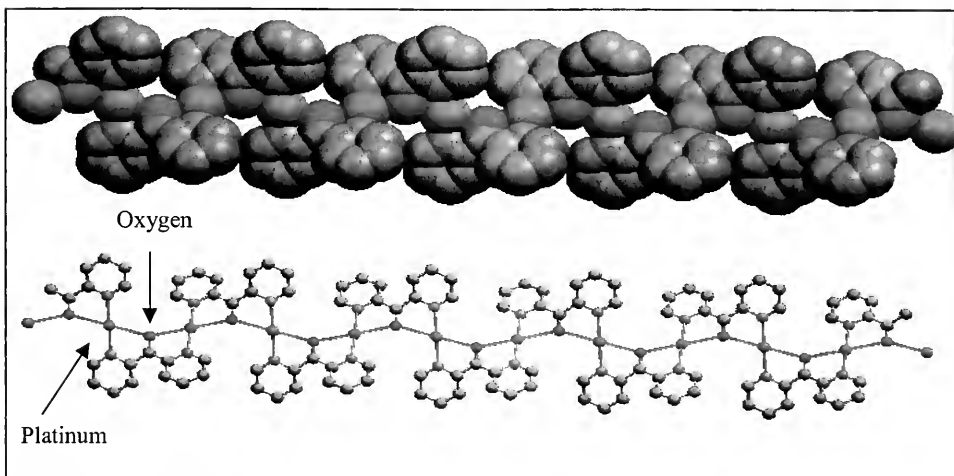
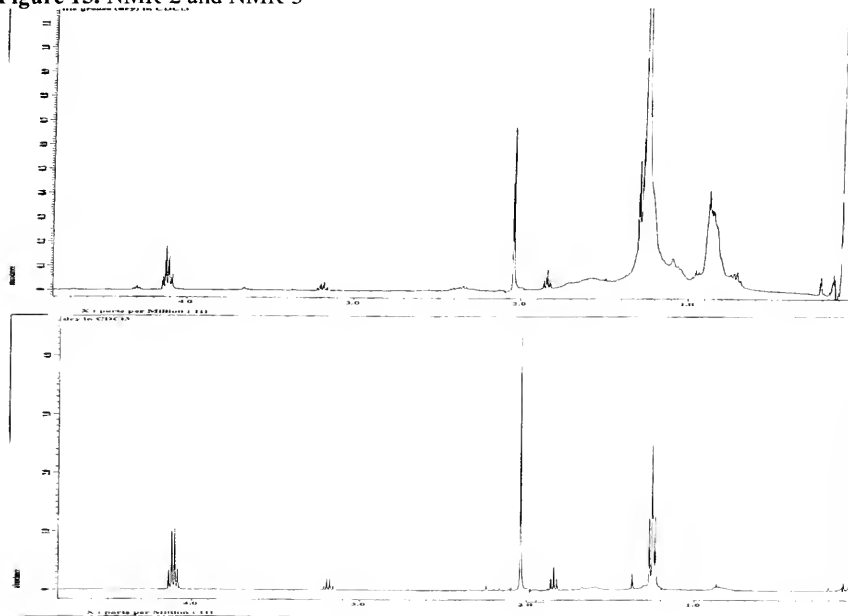


Figure 14. X-ray crystal structure of our polymer-dpk catalyst

Section 5.4: Most Recent Exploration of our [Pt(dpk)₂Cl₂]²⁺ catalyst

The most recent research has focused on a study of our $[\text{Pt}(\text{dpk})_2\text{Cl}_2]^{2+}$ catalyst, attempting to repeat the formation of oxalate and characterization of the product. Following the product extraction procedure (2), the sample was analyzed using ^1H -NMR (NMR-2). For the purposes of analyzing our esterified product, we wanted to make sure that the procedure was valid and successful. Thus, we also ran the esterification experiment with commercially obtained *trans*-1,2-cyclohexanedicarboxylic acid (see Sec 4.7). ^1H -NMR was also used for the analysis of this ester (NMR-3). When compared, these two NMR spectra are almost identical (Figure 15).

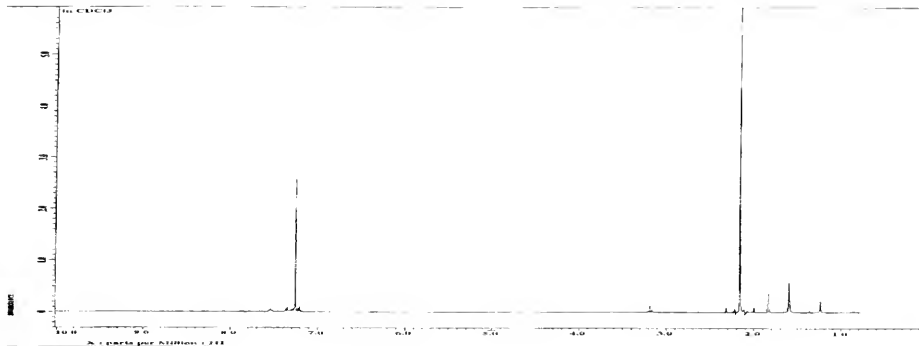
Figure 15. NMR-2 and NMR-3



The quartet at 4.1 ppm and the triplet at 1.3 ppm are strong evidence that we have repeated the electrocatalytical reduction CO_2 and made the simplest carbon-carbon bond – oxalate. We analyzed both products on GC/MS (GC/MS-3 and GC/MS-4), and these data are consistent with our ^1H -NMR data. The retention times are slightly different, which is probable when different solvents are used. However, then we wanted to make absolutely sure once again that what we made and esterified was undoubtedly oxalate, because the peaks for oxalate and ethyl acetate overlap in the ^1H -NMR. Since the extraction was done using ethyl acetate, there

were small but existing chances for traces of it remaining in our flasks. So we attempted the same esterification process, however, this time using chloroform instead of ethyl acetate. The final product was analyzed using ^1H -NMR (Figure 16).

Figure 16. NMR-4



The peaks for diethyl oxalate were omitted. This implies that our electrolysis product from the first esterification experiment was ethyl acetate instead of diethyl oxalate. However, due to the MS strong evidence of diethyl oxalate, and due to the fact that the product was dried *in vacuo* for a week before the NMR analysis, chances are that the second experiment using chloroform was not repeated completely in the same way.

SECTION 6: CONCLUSION

In conclusion, I have completed the study of the electrocatalytic reduction of CO₂ using our [Pt(dpk)Cl₄] catalyst. I have also completed the spectroscopic characterization of [Pt(dpk)₂Cl₂]²⁺, and began further exploration of the isolation and characterization of the electrolysis products. Further experiments need to be performed (see Section 7).

SECTION 7: FUTURE RESEARCH

This research could go in many directions. However, it is inevitable to repeat some of the experiments that led us to believe that we have formed oxalate. Since it is such an important reaction product in reducing CO₂, it would be useful to explore other ways of isolating the product, as well as focus on more in-depth NMR characterization. In the experiment where we tried to trap CO₂ with cyclohexene, it might be better to use the catalyst **2**, so the concentration of reduced CO₂ radical anions could be increased. It would be good to design a new cell that could have a greater flow of CO₂ through it without overflowing the cell. It would be also important to analyze the gas(es) produced during the course of the electrolysis experiment. Also, it would be immensely important to repeat experiments using our poly-dpk catalyst.

The ¹³CO₂ labeling study experiment should be repeated. If the peaks in the ¹³C-NMR spectrum reoccur again, a control experiment should be performed: this would consist of preparing two NMR samples with the same, known, amounts of phthalates in the same amounts of a solvent. If the peaks overlap, we will have enough evidence to support the making of those large organic molecules using CO₂ as the carbon source.

The GC/MS analysis that showed different retention times should be repeated, however, this time by injecting both samples at the same time. If only one peak is seen in the GC/MS spectrum, then we will have a strong evidence of the formation of oxalate.

REFERENCES

1. Yin X.; Moss J. R. *Coordination Chem. Rev.* **1999**, *181*, 27-59.
2. Kaneco, S.; Iiba, K.; Suzuki, S.; Ohta, K.; Mizuno, T. *J. Phys. Chem. B.* **1999**, *103*, 7456.
3. Mayer K; Castro-Rodriquez I. *Science*, **2004**, *305*, 1757-1759.
4. Darr J. A.; Poliakoff M. *Chem. Rev.* **1999**, *99*, 495-541.
5. Arakawa H.; Aresta M.; Armor J. N.; Barteau M. A.; Beckman E. J.; Bell A. T.; Bercaw J. E.; Creutz C.; Dinjus E.; Dixon D. A.; Domen K.; DuBois D. L.; Eckert J.; Fujita E.; Ginson D. H.; Goddard W. A.; Goodman D. W.; Keller J.; Kubas G. J.; Kung H. H.; Lyons J. E.; Manzer L. E.; Marks T. J.; Morokuma K.; Nicholas K. M.; Periana R.; Que L.; Rostrup-Nielson J.; Sachtler W. M. H.; Schmidt L. D.; Sen A.; Somorjai G. A.; Stair P. C.; Stults B. R.; Tumas W. *Chem. Rev.* **2001**, *101*, 953-996.
6. Grodkowski J.; Neta P. *J. Phys. Chem. A* **2000**, *104*, 1848-1853.
7. Hori Y.; Takahashi I.; Koga O.; Hoshi N. *J. Phys. Chem. B* **2002**, *106*, 15-17.
8. Rudolph M.; Dautz S.; Jager E. G. *J. Am. Chem. Soc.* **2000**, *122*, 10821-10830.
9. Teramura K.; Tanaka T.; Ishikawa H.; Kohno Y.; Funabiki T. *J. Phys. Chem. B* **2004**, *108*, 346-354.
10. Hayashi Y.; Kita S.; Brunschwig B. S.; Fujita E. *J. Am. Chem. Soc.* **2003**, *125*(39), 11976-11987.
11. Kobayashi T; Takahashi H. *Energy & Fuels* **2004**, *18*, 285-286.
12. Grodkowski J.; Neta P.; Fujita E.; Mahammed A.; Simkhovich L.; Gross Z. *J. Phys. Chem. A* **2002**, *106*, 4772-4778.
13. Stack, T.D.P.; Holm, R.H. *J. Am. Chem. Soc.* **1988**, *110*, 2484-2494
14. Osborne, R. R. and McWhinnie, W. R. *Inorg. Phys. Theor.*, **1967**, 2075-2078.
15. Feller, M. C. and Robson, R., *Aust. J. Chem.* **1968**, *21*, 2919-2927.
16. Feller, M. C. and Robson, R., *Aust. J. Chem.* **1970**, *23*, 1997-2003.
17. Bakker, I. J.; Feller, M. C.; Robson, R., *J. Inorg. Nucl. Chem.* **1971**, *33*, 747-754.
18. Ortego, J. D. and Perry, D. L., *J. Inorg. Nucl. Chem.* **1973**, *35*, 3031-3034.
19. Rattanaphani, V. and McWhinnie, W. R. *Inorg. Chim. Acta* **1974**, *9*, 239-244.
20. Perry, D. L.; Vaz, C.; Wendlandt, W. W. *Thermochimica Acta* **1974**, *9*, 76-78.
21. Fischer, B. E. and Sigel, H. *J. Inorg. Nucl. Chem.* **1975**, *37*, 2127-2132.

22. Wang, S.; Richardson, Jr., J. W.; Briggs, S. J.; Jacobson, R. A.; Jensen, W. P. *Inorg. Chim. Acta* **1986**, *111*, 67-72.
23. Ishaq, M; Baghlaf, A. O.; Al-Mouty, A.; Al-Dousry, M., *J. Chem. Soc. Pak.* **1992**, *14*, 115-117.
24. Ortego, J. D.; Waters, D. D.; Steele, C. S. *J. Inorg. Nucl. Chem.* **1974**, *36*, 751-756.
25. Ortego, J. D.; Upalawanna, S.; Amanollahi, S. *J. Inorg. Nucl. Chem.* **1979**, *41*, 593-595.
26. Basu, A.; Saple, A. R.; Sapre, N. Y. *J. Chem. Soc. Dalton Trans.* **1987**, 1797-1799.
27. Sommerer, S. O.; Jensen, W. P.; Jacobson, R. A. *Inorg. Chim. Acta* **1990**, *172*, 3-11.
28. Bhaduri, S.; Sapre, N. Y.; Jones, P. G. *J. Chem. Soc. Dalton Trans.* **1991**, 2539-2543.
29. Kavounis, C. A.; Tsiamis, C.; Cardin, C. J.; Zubavichus, Y. *Polyhedron* **1996**, *15*, 385-390.
30. Goher, M. A. S.; Al-Salem, N. A.; Mak, T. C. W. *Polyhedron* **2000**, *19*, 1465-1470.
31. Parker, O. J.; Aubol, S. L.; Breneman, G. L. *Polyhedron* **2000**, *19*, 623-626.
32. Basu, A.; Kasar, T. G.; Sapre, N. Y. *Inorg. Chem.* **1988**, *27*, 4539-4542.
33. Bandoli, G.; Dolmella, A.; Gerber, T. I.A.; du Preez, J. G.H.; Kemp, H. J. *Inorg. Chim. Acta*, **1994**, *217*, 141-147.
34. a. Bakir, M. and McKenzie, J. A. M., *J. Electroanalytical Chem.*, **1997**, *425*, 61-66. b. Bakir, M. and McKenzie, J. A. M. *J. Chem. Soc., Dalton Trans.* **1997**, 3571-3578.
35. Yang, G; Zheng, S-L.; Chen, X-M.; Lee, H. K.; Zhou, Z-Y.; Mak, T. C.W. *Inorg. Chim. Acta* **2000**, *303*, 86-93.
36. Alonzo, G.; Bertazzi, N.; Maggio, F.; Benetollo, F.; Bombieri, G. *Polyhedron*, **1996**, *15*, 4269-4273.
37. Annibale, G.; Canovese, L.; Cattalini, L.; Natile, G.; Biagini-Cingi, M.; Manotti-Lanferdi, A. *J. Chem. Soc. Dalton Trans.*, **1981**, 2280-2287.
38. Ferreira, A. D. Q.; Bino, A.; Gibson, D. *Inorg. Chim. Acta* **1997**, *265*, 155-161.
39. Crowder K. N.; Garcia S. J.; Burr R. L.; North J. M.; Wilson M. H.; Conley B. L.; Fanwick P. E.; White P. S.; Sienerth K. D.; Granger, II R. M. *Inorg. Chem.* **2004**, *43*(1) 72-78.
40. Perry, D. L.; Margrave, J. L.; Bonnell, D. W. *Inorg. Chim. Acta* **1985**, *101*, L1-L4.41. Burr, R. Senior Honors Thesis, Sweet Briar College, 2001. "What To Do With the CO₂?"
42. a) Ratliff, K.S. Ph.D. Dissertation, Purdue University, 1990. b) Morgenstern, D. A, Wittrig, R. E, Fanwick, P. E., Kubiak, C. P., *J. Am. Chem. Soc.*, **1993**, *115*, 6470-6471
43. Eggins, B.R.; Ennis, C.; McConnell, R.; Spence, M. *J. Appl. Electrochem.* **1997**, *27*, 706

44. Nagao H.; Mizukawa T.; Tanaka K. *Inorg. Chem.* **2000**, *104*, 1848-1853.
45. Simon-Manso, E.; Kubiak, C.P. *Organometallics* **2005**, *24*, 96-102
46. Emma Kate Payne, Senior Honors Thesis, Sweet Briar College, **2003**

Appendix A

X-ray crystallographic data of $[\text{Pt}(\text{dpk})_2\text{Cl}_2]^{2+}$

Cif file for Pt(dpk)₂Cl₂ dihydrate.

```
#####  
data_global  
#####  
_audit_creation_date      29-06-04  
_audit_creation_method  
  SHELXL_and_local_programs  
_audit_update_record
```

1. SUBMISSION DETAILS

```
_publ_contact_author_name  'Phillip E. Fanwick'  
_publ_contact_author_address  
; Department of Chemistry  
  Purdue University  
  560 Oval Dr.  
  W. Lafayette  
  IN 47907-2084  
  USA  
;  
_publ_contact_author_email  'pfanwick@purdue.edu'  
_publ_contact_author_fax    '1(765)4940239'  
_publ_contact_author_phone  '1(765)4944572'
```

3. TITLE AND AUTHOR LIST

```
'GRANGER'  
; Department of Chemistry  
  Purdue University  
  W. Lafayette  
  IN 47907  
  USA  
;  
  
'FANWICK, PHILLIP E.'  
; Department of Chemistry  
  Purdue University  
  W. Lafayette  
  IN 47907  
  USA
```

References

Burla, M.C., Camalli, M., Carrozzini, B., Cascarano, G.L., Giacovazzo, C., Polidori, G., Spagna R. (2003). J. Appl. Cryst., 36, 1103

Enraf-Nonius (1993), CAD4 Express, Enraf-Nonius, Delft, The Netherlands.

Johnson, C.K. (1976). ORTEP. Report ORNL-5138. Oak Ridge National Laboratory, Tennessee, USA.

Cif file for Pt(dpk)₂Cl₂ dihydrate.

Nonius(1998), Collect Users Manual, Nonius Delft, The Netherlands.

Otwinowski Z. & Minor, W. (1997). Methods Enzymol., 276, 307-327.

Sheldrick, G.M. (1997). SHELXL97, Program for the Refinement of Crystal Structures. Univ. of Göttingen, Germany.

Spek A.L.(1997) PLATON. Program. Univ. of Utrecht, The Netherlands

data_ACB324

4 CRYSTAL DATA

```
_chemical_compound_source      ?
_exptl_crystal_description     plate
_exptl_crystal_colour_primary  colourless
_exptl_crystal_size_max       0.35
_exptl_crystal_size_mid       0.30
_exptl_crystal_size_min       0.23
_chemical_name_systematic
; ?
_exptl_crystal_density_method  ?

_chemical_formula_sum          'C26 H22 F12 N6 O4 P2 Pt1'
_chemical_formula_moiety       'C22 H16 N4 O4 Pt1,2(F6 P1),2(C2 H3 N1)'
_chemical_formula_structural   ?
_chemical_formula_weight       967.52
_symmetry_cell_setting         triclinic
_symmetry_space_group_name_Hall '-P 1'
_symmetry_space_group_name_H-M 'P -1'
loop_
_symmetry_equiv_pos_as_xyz
  'x, y, z'
  '-x, -y, -z'

_cell_length_a                 7.1850(6)
_cell_length_b                 10.7561(18)
_cell_length_c                 10.9989(13)
_cell_angle_alpha              76.948(8)
_cell_angle_beta               89.190(6)
_cell_angle_gamma              86.304(8)
_cell_volume                   826.34(18)
_cell_measurement_reflns_used  11025
_cell_measurement_theta_min    3
_cell_measurement_theta_max    27
_cell_formula_units_z          1
```


Cif file for Pt(dpk)₂Cl₂ dihydrate.

_exptl_crystal_density_diffn 1.94
_exptl_crystal_density_meas ?
loop_
_atom_type_symbol
_atom_type_radius_bond
Pt 1.30
P 1.06
F 0.72
O 0.73
N 0.75
C 0.77
H 0.32

_diffn_radiation_type MO-K α
_diffn_radiation_wavelength 0.71073
_exptl_absorpt_coefficient_mu 4.491
_cell_measurement_temperature 193
_exptl_crystal_F_000 468

5 DATA COLLECTION

_diffn_ambient_temperature 193
_diffn_measurement_device_type Nonius_KappaCCD
_diffn_radiation_monochromator 'graphite 002'
_diffn_measurement_method \w
_exptl_absorpt_correction_type multi-scan_(Otwinowski_&_Minor,_1997
_exptl_absorpt_correction_T_min 0.3468
_exptl_absorpt_correction_T_max 0.3640
_diffn_reflns_number 11025
_diffn_measured_fraction_theta_max 0.9690
_diffn_reflns_theta_full 24.4
_diffn_measured_fraction_theta_full 1.0000
_reflns_number_total 3892
_reflns_number_gt 3872
_reflns_threshold_expression >2.0\sigma(I)
_diffn_reflns_av_R_equivalents 0.070
_diffn_reflns_theta_min 3.01
_diffn_reflns_theta_max 27.99
_diffn_reflns_limit_h_min 0
_diffn_reflns_limit_k_min -14
_diffn_reflns_limit_l_min -14
_diffn_reflns_limit_h_max 9
_diffn_reflns_limit_k_max 14
_diffn_reflns_limit_l_max 14
_diffn_special_details 'mosaicity from Denzo/Scalepack is 0.85'

Cif file for Pt(dpk)₂Cl₂ dihydrate.

6 REFINEMENT DATA

_refine_special_details

;

Refinement on F^2 for ALL reflections except for 0 with very negative F^2 or flagged by the user for potential systematic errors. Weighted R-factors wR and all goodnesses of fit S are based on F^2 , conventional R-factors R are based on F, with F set to zero for negative F^2 . The observed criterion of $F^2 > 2\sigma(F^2)$ is used only for calculating R_factor_obs etc. and is not relevant to the choice of reflections for refinement. R-factors based on F^2 are statistically about twice as large as those based on F, and R-factors based on ALL data will be even larger.

_refine_ls_structure_factor_coef Fsqd

_refine_ls_matrix_type full

_refine_ls_R_factor_all 0.039

_refine_ls_R_factor_gt 0.039

_refine_ls_wR_factor_ref 0.092

_refine_ls_wR_factor_gt 0.092

_refine_ls_hydrogen_treatment constr

_refine_ls_number_reflns 3890

_refine_ls_number_parameters 279

_refine_ls_number_restraints 0

_refine_ls_goodness_of_fit_ref 1.082

_refine_ls_weighting_scheme 'calc'

_refine_ls_weighting_details

'1/[\sigma^2(Fo^2)+(0.0618P)^2+0.3153P] where $P=(Fo^2+2Fc^2)/3$ '

_refine_ls_shift/su_max 0.000

_refine_diff_density_max 1.17

_refine_diff_density_min -3.18

_refine_ls_extinction_method none

_atom_type_scatter_source

'International Tables for Crystallography (Vol C)'

7 COMPUTING DATA

_computing_data_collection Collect_(Nonius,_1998)

_computing_cell_refinement DENZO/SCALEPACK_(Otwinowski,_1996)

_computing_data_reduction DENZO/SCALEPACK_(Otwinowski,_1996)

_computing_structure_solution Direct_methods_(SIR2002,_Burla_et_al.,_2003)

_computing_structure_refinement SHELX97_(Sheldrick,_1997)

_computing_molecular_graphics

;

ORTEP (Johnson, 1976)

PLATON (Spek, 1997)

;

Cif file for Pt(dpk)₂Cl₂ dihydrate.

8 ATOMIC COORDINATES AND THERMAL PARAMETERS

loop_
_atom_site_label
_atom_site_type_symbol
_atom_site_fract_x
_atom_site_fract_y
_atom_site_fract_z
_atom_site_U_iso_or_equiv
_atom_site_adp_type
_atom_site_occupancy
_atom_site_symmetry_multiplicity
_atom_site_calc_flag
_atom_site_refinement_flags
_atom_site_disorder_assembly
_atom_site_disorder_group

Pt Pt 0.5000 0.5000 0.5000 0.02572(9) Uani 1 2 d S . .
P P 0.0658(3) 0.2518(2) 0.19244(15) 0.0641(5) Uani 1 1 d . . .
F(1) F 0.0540(8) 0.2368(7) 0.0559(4) 0.0934(18) Uani 1 1 d . A .
F(2A) F -0.133(3) 0.292(2) 0.211(3) 0.106(9) Uani 0.51(2) 1 d P A 1
F(2B) F -0.157(3) 0.247(3) 0.196(2) 0.099(9) Uani 0.49(2) 1 d P A 2
F(3A) F -0.001(3) 0.0980(18) 0.227(2) 0.130(8) Uani 0.51(2) 1 d P A 1
F(3B) F 0.086(3) 0.1306(17) 0.2695(16) 0.118(8) Uani 0.49(2) 1 d P A 2
F(4A) F 0.1082(17) 0.217(2) 0.3419(8) 0.092(6) Uani 0.51(2) 1 d P A 1
F(4B) F 0.041(3) 0.319(2) 0.3106(14) 0.104(7) Uani 0.49(2) 1 d P A 2
F(5A) F 0.280(2) 0.176(3) 0.1839(15) 0.133(9) Uani 0.51(2) 1 d P A 1
F(5B) F 0.2693(17) 0.290(3) 0.1769(9) 0.100(8) Uani 0.49(2) 1 d P A 2
F(6A) F 0.158(5) 0.370(2) 0.1720(18) 0.152(13) Uani 0.51(2) 1 d P A 1
F(6B) F 0.015(2) 0.4077(14) 0.1049(16) 0.105(6) Uani 0.49(2) 1 d P A 2
O(11) O 0.2287(4) 0.4909(3) 0.4694(3) 0.0333(7) Uani 1 1 d . . .
O(12) O 0.0055(5) 0.6271(4) 0.3459(4) 0.0431(9) Uani 1 1 d . . .
N(11) N 0.5095(5) 0.4377(4) 0.6888(3) 0.0299(8) Uani 1 1 d . . .
N(21) N 0.5939(6) 0.3217(4) 0.4869(3) 0.0306(8) Uani 1 1 d . . .
N(91) N 0.3826(16) 0.1472(9) 0.7119(9) 0.106(3) Uani 1 1 d . . .
C(1) C 0.1871(6) 0.6107(5) 0.3834(4) 0.0343(10) Uani 1 1 d . . .
C(12) C 0.3703(7) 0.4491(5) 0.7696(4) 0.0345(10) Uani 1 1 d . . .
C(13) C 0.4024(8) 0.4059(6) 0.8957(5) 0.0429(12) Uani 1 1 d . . .
C(14) C 0.5783(9) 0.3536(6) 0.9376(5) 0.0450(12) Uani 1 1 d . . .
C(15) C 0.7204(8) 0.3450(6) 0.8519(5) 0.0407(11) Uani 1 1 d . . .
C(16) C 0.6817(7) 0.3880(5) 0.7278(4) 0.0329(9) Uani 1 1 d . . .
C(22) C 0.5153(7) 0.2496(5) 0.4215(4) 0.0367(10) Uani 1 1 d . . .
C(23) C 0.5974(9) 0.1294(6) 0.4210(5) 0.0444(12) Uani 1 1 d . . .
C(24) C 0.7576(8) 0.0876(5) 0.4924(6) 0.0459(12) Uani 1 1 d . . .
C(25) C 0.8358(8) 0.1656(6) 0.5591(5) 0.0421(11) Uani 1 1 d . . .
C(26) C 0.7518(6) 0.2842(5) 0.5526(4) 0.0334(9) Uani 1 1 d . . .

Cif file for Pt(dpk)₂Cl₂ dihydrate.

C(92) C 0.3285(14) 0.0939(8) 0.7999(9) 0.075(2) Uani 1 1 d . . .
C(93) C 0.255(3) 0.0237(18) 0.9169(15) 0.191(11) Uani 1 1 d . . .
H(12) H 0.2514 0.4865 0.7400 0.041 Uiso 1 1 calc R . .
H(13) H 0.3049 0.4119 0.9537 0.051 Uiso 1 1 calc R . .
H(14) H 0.6014 0.3238 1.0244 0.054 Uiso 1 1 calc R . .
H(15) H 0.8415 0.3100 0.8792 0.049 Uiso 1 1 calc R . .
H(22) H 0.4041 0.2799 0.3756 0.044 Uiso 1 1 calc R . .
H(23) H 0.5458 0.0769 0.3730 0.053 Uiso 1 1 calc R . .
H(24) H 0.8135 0.0045 0.4953 0.055 Uiso 1 1 calc R . .
H(25) H 0.9449 0.1374 0.6079 0.050 Uiso 1 1 calc R . .
H(93A) H 0.3010 0.0573 0.9858 0.286 Uiso 1 1 calc R . .
H(93B) H 0.2949 -0.0670 0.9292 0.286 Uiso 1 1 calc R . .
H(93C) H 0.1181 0.0335 0.9150 0.286 Uiso 1 1 calc R . .

loop_

_atom_site_aniso_label
_atom_site_aniso_U_11
_atom_site_aniso_U_22
_atom_site_aniso_U_33
_atom_site_aniso_U_12
_atom_site_aniso_U_13
_atom_site_aniso_U_23

Pt 0.02402(13) 0.02763(14) 0.02577(12) -0.00193(8) -0.00146(7) -0.00636(8)
P 0.0535(9) 0.1009(16) 0.0401(7) -0.0284(10) -0.0001(6) -0.0137(8)
F(1) 0.095(4) 0.135(5) 0.055(2) -0.020(4) -0.009(2) -0.028(3)
F(2A) 0.090(15) 0.103(14) 0.105(13) 0.047(12) 0.017(11) 0.004(11)
F(2B) 0.058(7) 0.16(2) 0.066(8) -0.043(12) -0.005(6) 0.007(11)
F(3A) 0.170(18) 0.089(11) 0.134(14) -0.057(11) -0.010(11) -0.018(9)
F(3B) 0.160(16) 0.066(10) 0.091(11) 0.042(10) 0.019(10) 0.044(9)
F(4A) 0.072(7) 0.163(17) 0.037(4) -0.053(8) 0.000(4) -0.002(6)
F(4B) 0.124(12) 0.140(16) 0.064(8) -0.055(11) 0.028(7) -0.044(9)
F(5A) 0.061(7) 0.24(3) 0.095(9) 0.037(11) -0.010(6) -0.037(13)
F(5B) 0.045(6) 0.21(2) 0.035(4) -0.033(9) -0.003(4) -0.011(8)
F(6A) 0.27(3) 0.099(14) 0.112(13) -0.125(19) 0.076(18) -0.043(11)
F(6B) 0.120(11) 0.078(8) 0.099(10) 0.005(7) 0.013(8) 0.017(7)
O(11) 0.0253(15) 0.0382(19) 0.0336(15) -0.0023(13) 0.0023(11) -0.0022(13)
O(12) 0.0267(17) 0.055(2) 0.0436(19) -0.0014(15) -0.0082(13) -0.0021(17)
N(11) 0.0318(19) 0.0273(19) 0.0300(17) -0.0042(14) -0.0014(13) -0.0043(14)
N(21) 0.0335(19) 0.030(2) 0.0284(17) -0.0033(15) -0.0016(14) -0.0071(14)
N(91) 0.160(9) 0.068(5) 0.100(6) -0.032(5) 0.057(6) -0.035(5)
C(1) 0.028(2) 0.039(3) 0.035(2) -0.0014(18) -0.0028(16) -0.0078(19)
C(12) 0.037(2) 0.039(3) 0.031(2) -0.0041(19) 0.0052(17) -0.0138(18)
C(13) 0.052(3) 0.044(3) 0.036(2) -0.009(2) 0.006(2) -0.013(2)
C(14) 0.059(3) 0.045(3) 0.030(2) -0.005(2) -0.005(2) -0.006(2)
C(15) 0.041(3) 0.044(3) 0.037(2) -0.003(2) -0.0073(19) -0.009(2)
C(16) 0.032(2) 0.035(2) 0.032(2) -0.0050(18) -0.0049(16) -0.0066(18)

Cif file for Pt(dpk)₂Cl₂ dihydrate.

C(22) 0.037(2) 0.040(3) 0.034(2) -0.0051(19) 0.0008(17) -0.0097(19)
C(23) 0.055(3) 0.035(3) 0.047(3) -0.005(2) 0.006(2) -0.017(2)
C(24) 0.049(3) 0.031(3) 0.056(3) 0.007(2) 0.010(2) -0.009(2)
C(25) 0.040(3) 0.042(3) 0.040(2) 0.006(2) 0.0028(19) -0.004(2)
C(26) 0.030(2) 0.037(3) 0.032(2) 0.0012(17) 0.0016(16) -0.0058(18)
C(92) 0.097(6) 0.055(4) 0.083(5) -0.017(4) 0.022(5) -0.033(4)
C(93) 0.33(3) 0.139(15) 0.128(12) -0.116(17) 0.101(16) -0.054(11)

9 MOLECULAR GEOMETRY

_geom_special_details

;

All esds (except the esd in the dihedral angle between two l.s. planes) are estimated using the full covariance matrix. The cell esds are taken into account individually in the estimation of esds in distances, angles and torsion angles; correlations between esds in cell parameters are only used when they are defined by crystal symmetry. An approximate (isotropic) treatment of cell esds is used for estimating esds involving l.s. planes.

Bond Distances:

Pt O(11) 1.995(3) . 2_666 ?	N(11) C(12) 1.346(6) . . ?
Pt O(11) 1.995(3) . . ?	N(11) C(16) 1.352(6) . . ?
Pt N(21) 2.027(4) . 2_666 ?	N(21) C(22) 1.326(7) . . ?
Pt N(21) 2.027(4) . . ?	N(21) C(26) 1.344(6) . . ?
Pt N(11) 2.034(4) . . ?	N(91) C(92) 1.088(11) . . ?
Pt N(11) 2.034(4) . 2_666 ?	C(1) C(16) 1.531(7) . 2_666 ?
P F(3B) 1.386(11) . . ?	C(1) C(26) 1.548(7) . 2_666 ?
P F(6A) 1.438(12) . . ?	C(12) C(13) 1.377(7) . . ?
P F(2A) 1.49(2) . . ?	C(13) C(14) 1.391(9) . . ?
P F(5B) 1.541(11) . . ?	C(14) C(15) 1.393(8) . . ?
P F(1) 1.551(5) . . ?	C(15) C(16) 1.366(7) . . ?
P F(2B) 1.61(2) . . ?	C(16) C(1) 1.531(7) . 2_666 ?
P F(4B) 1.626(13) . . ?	C(22) C(23) 1.388(8) . . ?
P F(4A) 1.630(9) . . ?	C(23) C(24) 1.394(9) . . ?
P F(5A) 1.702(15) . . ?	C(24) C(25) 1.381(9) . . ?
P F(3A) 1.710(16) . . ?	C(25) C(26) 1.363(8) . . ?
P F(6B) 1.753(13) . . ?	C(26) C(1) 1.548(7) . 2_666 ?
O(11) C(1) 1.433(6) . . ?	C(92) C(93) 1.450(15) . . ?
O(12) C(1) 1.363(6) . . ?	

Bond Angles:

O(11) Pt O(11) 180(2000) 2_666 . . ?
 O(11) Pt N(21) 99.84(16) 2_666 . 2_666 ?
 O(11) Pt N(21) 80.16(16) . . 2_666 ?
 O(11) Pt N(21) 80.16(16) 2_666 . . ?
 O(11) Pt N(21) 99.84(16) . . ?
 N(21) Pt N(21) 180.0(2) 2_666 . . ?
 O(11) Pt N(11) 79.56(14) 2_666 . . ?
 O(11) Pt N(11) 100.44(14) . . ?
 N(21) Pt N(11) 91.88(16) 2_666 . . ?
 N(21) Pt N(11) 88.12(16) . . ?
 O(11) Pt N(11) 100.44(14) 2_666 . 2_666 ?
 O(11) Pt N(11) 79.56(14) . . 2_666 ?
 N(21) Pt N(11) 88.12(16) 2_666 . 2_666 ?
 N(21) Pt N(11) 91.88(16) . . 2_666 ?
 N(11) Pt N(11) 180.000(2) . . 2_666 ?
 F(3B) P F(6A) 137.7(17) . . ?
 F(3B) P F(2A) 103.2(12) . . ?
 F(6A) P F(2A) 103.3(16) . . ?
 F(3B) P F(5B) 102.0(12) . . ?
 F(6A) P F(5B) 44.2(11) . . ?
 F(2A) P F(5B) 147.2(14) . . ?
 F(3B) P F(1) 107.9(11) . . ?
 F(6A) P F(1) 99.6(7) . . ?
 F(2A) P F(1) 99.2(11) . . ?
 F(5B) P F(1) 92.8(5) . . ?
 F(3B) P F(2B) 90.9(13) . . ?
 F(6A) P F(2B) 122.9(17) . . ?
 F(2A) P F(2B) 21.6(15) . . ?
 F(5B) P F(2B) 166.7(13) . . ?
 F(1) P F(2B) 86.3(9) . . ?
 F(3B) P F(4B) 92.3(10) . . ?
 F(6A) P F(4B) 68.2(8) . . ?
 F(2A) P F(4B) 68.2(12) . . ?
 F(5B) P F(4B) 90.1(9) . . ?
 F(1) P F(4B) 158.5(10) . . ?
 F(2B) P F(4B) 86.1(10) . . ?
 F(3B) P F(4A) 53.4(10) . . ?
 F(6A) P F(4A) 93.1(10) . . ?
 F(2A) P F(4A) 92.5(12) . . ?
 F(5B) P F(4A) 85.8(5) . . ?
 F(1) P F(4A) 160.2(9) . . ?
 F(2B) P F(4A) 99.5(9) . . ?
 F(4B) P F(4A) 41.3(7) . . ?
 F(3B) P F(5A) 66.1(11) . . ?
 F(6A) P F(5A) 87.5(14) . . ?
 F(2A) P F(5A) 168.7(13) . . ?
 F(5B) P F(5A) 43.4(9) . . ?
 F(1) P F(5A) 81.8(6) . . ?
 F(2B) P F(5A) 148.9(13) . . ?
 F(4B) P F(5A) 114.1(10) . . ?
 F(4A) P F(5A) 83.7(9) . . ?
 F(3B) P F(3A) 32.2(11) . . ?
 F(6A) P F(3A) 168.5(17) . . ?
 F(2A) P F(3A) 87.0(12) . . ?
 F(5B) P F(3A) 124.9(13) . . ?
 F(1) P F(3A) 83.5(8) . . ?
 F(2B) P F(3A) 68.2(12) . . ?
 F(4B) P F(3A) 112.1(10) . . ?
 F(4A) P F(3A) 81.2(8) . . ?
 F(5A) P F(3A) 81.9(13) . . ?
 F(3B) P F(6B) 173.1(9) . . ?
 F(6A) P F(6B) 45.2(13) . . ?
 F(2A) P F(6B) 70.2(11) . . ?
 F(5B) P F(6B) 83.6(9) . . ?
 F(1) P F(6B) 75.6(7) . . ?
 F(2B) P F(6B) 83.4(10) . . ?
 F(4B) P F(6B) 83.6(9) . . ?
 F(4A) P F(6B) 123.7(10) . . ?
 F(5A) P F(6B) 120.7(10) . . ?
 F(3A) P F(6B) 145.7(9) . . ?
 C(1) O(11) Pt 101.4(3) . . ?
 C(12) N(11) C(16) 122.0(4) . . ?
 C(12) N(11) Pt 126.6(3) . . ?
 C(16) N(11) Pt 111.3(3) . . ?
 C(22) N(21) C(26) 122.9(5) . . ?
 C(22) N(21) Pt 125.9(3) . . ?
 C(26) N(21) Pt 111.1(3) . . ?
 O(12) C(1) O(11) 112.8(4) . . ?
 O(12) C(1) C(16) 111.0(4) . . 2_666 ?
 O(11) C(1) C(16) 106.0(4) . . 2_666 ?
 O(12) C(1) C(26) 113.6(4) . . 2_666 ?
 O(11) C(1) C(26) 106.5(4) . . 2_666 ?
 C(16) C(1) C(26) 106.4(4) 2_666 . 2_666 ?
 N(11) C(12) C(13) 119.2(5) . . ?
 C(12) C(13) C(14) 119.6(5) . . ?
 C(13) C(14) C(15) 119.9(5) . . ?
 C(16) C(15) C(14) 118.4(5) . . ?
 N(11) C(16) C(15) 120.8(5) . . ?
 N(11) C(16) C(1) 110.9(4) . . 2_666 ?
 C(15) C(16) C(1) 128.3(5) . . 2_666 ?

Cif file for Pt(dpk)₂Cl₂ dihydrate.

N(21) C(22) C(23) 119.1(5) ... ?
C(22) C(23) C(24) 118.5(5) ... ?
C(25) C(24) C(23) 120.7(5) ... ?
C(26) C(25) C(24) 118.0(5) ... ?

N(21) C(26) C(25) 120.7(5) ... ?
N(21) C(26) C(1) 111.4(4) ... 2_666 ?
C(25) C(26) C(1) 128.0(5) ... 2_666 ?
N(91) C(92) C(93) 179.4(16) ... ?

Torsion Angles:

O(11) Pt O(11) C(1) -44(33) 2_666 ... ?
N(21) Pt O(11) C(1) 44.9(3) 2_666 ... ?
N(21) Pt O(11) C(1) -135.1(3) ... ?
N(11) Pt O(11) C(1) 135.0(3) ... ?
N(11) Pt O(11) C(1) -45.0(3) 2_666 ... ?
O(11) Pt N(11) C(12) 151.9(4) 2_666 ... ?
O(11) Pt N(11) C(12) -28.1(4) ... ?
N(21) Pt N(11) C(12) 52.3(4) 2_666 ... ?
N(21) Pt N(11) C(12) -127.7(4) ... ?
N(11) Pt N(11) C(12) -170(36) 2_666 ... ?
O(11) Pt N(11) C(16) -24.2(3) 2_666 ... ?
O(11) Pt N(11) C(16) 155.8(3) ... ?
N(21) Pt N(11) C(16) -123.9(3) 2_666 ... ?
N(21) Pt N(11) C(16) 56.1(3) ... ?
N(11) Pt N(11) C(16) 14(36) 2_666 ... ?
O(11) Pt N(21) C(22) -153.2(4) 2_666 ... ?
O(11) Pt N(21) C(22) 26.8(4) ... ?
N(21) Pt N(21) C(22) 82(18) 2_666 ... ?
N(11) Pt N(21) C(22) 127.1(4) ... ?
N(11) Pt N(21) C(22) -52.9(4) 2_666 ... ?
O(11) Pt N(21) C(26) 25.8(3) 2_666 ... ?
O(11) Pt N(21) C(26) -154.2(3) ... ?
N(21) Pt N(21) C(26) -99(18) 2_666 ... ?
N(11) Pt N(21) C(26) -53.9(3) ... ?
N(11) Pt N(21) C(26) 126.1(3) 2_666 ... ?
Pt O(11) C(1) O(12) 179.2(4) ... ?

Pt O(11) C(1) C(16) 57.5(4) ... 2_666 ?
Pt O(11) C(1) C(26) -55.5(4) ... 2_666 ?
C(16) N(11) C(12) C(13) -1.7(8) ... ?
Pt N(11) C(12) C(13) -177.5(4) ... ?
N(11) C(12) C(13) C(14) 1.2(8) ... ?
C(12) C(13) C(14) C(15) -0.1(9) ... ?
C(13) C(14) C(15) C(16) -0.4(9) ... ?
C(12) N(11) C(16) C(15) 1.1(8) ... ?
Pt N(11) C(16) C(15) 177.5(4) ... ?
C(12) N(11) C(16) C(1) -178.7(4) ... 2_666 ?
Pt N(11) C(16) C(1) -2.4(5) ... 2_666 ?
C(14) C(15) C(16) N(11) 0.0(8) ... ?
C(14) C(15) C(16) C(1) 179.8(5) ... 2_666 ?
C(26) N(21) C(22) C(23) 0.6(7) ... ?
Pt N(21) C(22) C(23) 179.5(4) ... ?
N(21) C(22) C(23) C(24) 1.7(8) ... ?
C(22) C(23) C(24) C(25) -2.0(8) ... ?
C(23) C(24) C(25) C(26) 0.0(8) ... ?
C(22) N(21) C(26) C(25) -2.7(7) ... ?
Pt N(21) C(26) C(25) 178.3(4) ... ?
C(22) N(21) C(26) C(1) 178.6(4) ... 2_666 ?
Pt N(21) C(26) C(1) -0.5(5) ... 2_666 ?
C(24) C(25) C(26) N(21) 2.3(7) ... ?
C(24) C(25) C(26) C(1) -179.1(5) ... 2_666 ?

Appendix B

NMR and GC/MS Spectra

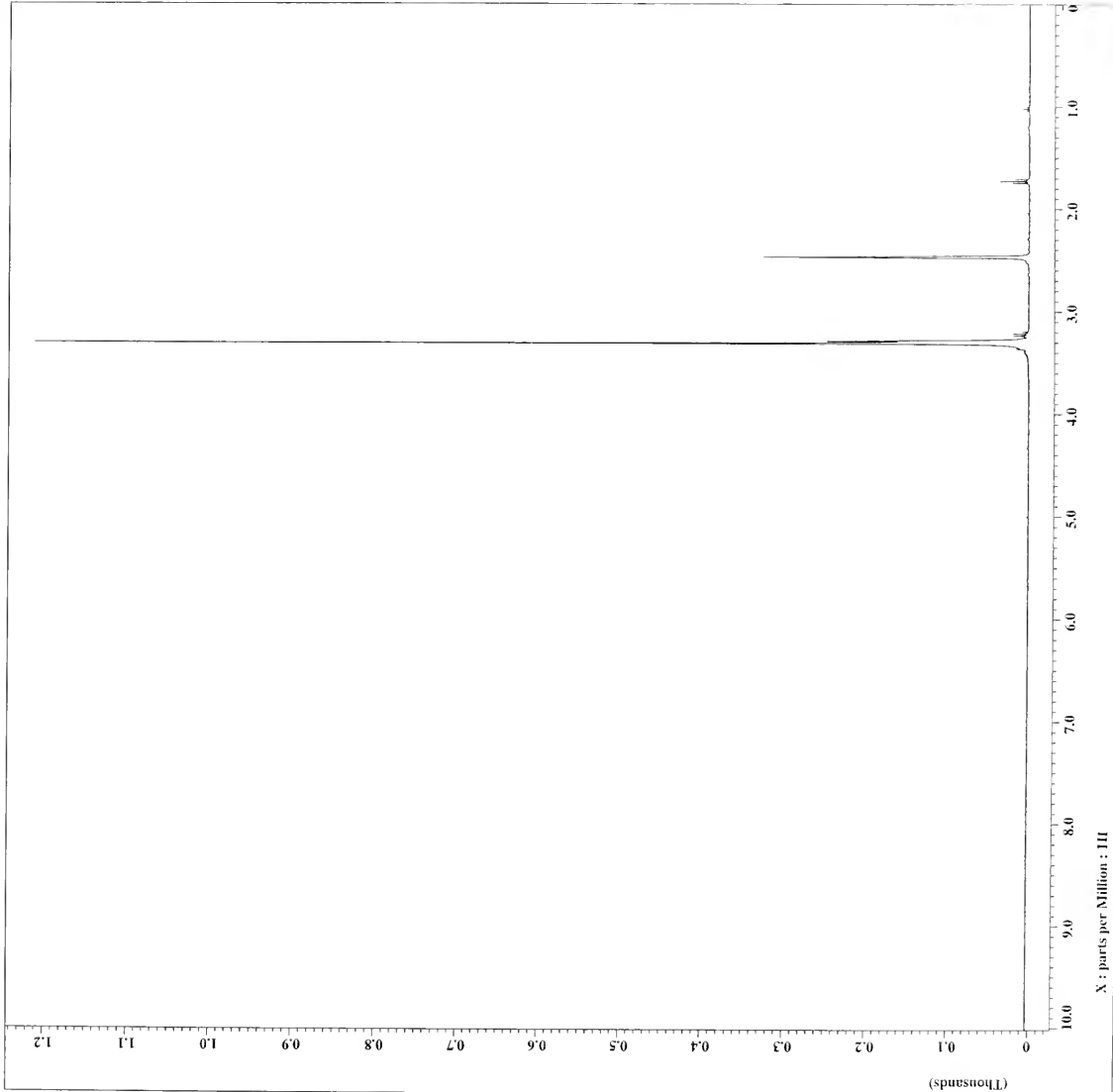


Filename = ac-bt-15 1h-3.jdf
Authent = NMRSEARCHES
Experiment = single_pulse.ex2
Sample_id = ac-bt-15
Solvent = DMSO-D6
Creation_time = 9-NOV-2004 13:58:17
Revision_time = 25-APR-2005 13:50:53
Current_time = 25-APR-2005 13:50:57

Data_format = 1D_COMPLEX
Dim_size = 13107
Dim_title = 1H
Dim_units = [ppm]
Dimensions = X
Site = ECX 400
Spectrometer = DELTA2_NMR

Field_strength = 9.389765[T] (400[MHz])
X_acq_duration = 2.18365952[s]
X_domain = 1H.18365952[s]
X_freq = 399.78219838[MHz]
X_offset = 5[ppm]
X_points = 16384
X_prescans = 1
X_resolution = 0.45794685[Hz]
X_resolution_ppm = 1H.5030012[MHz]
Xrr_domain = 1H
Xrr_freq = 399.78219838[MHz]
Xrr_offset = 5[ppm]
Tri_domain = 1H
Tri_freq = 399.78219838[MHz]
Tri_offset = 5[ppm]
Xod_return = 1
Stops = 16
Total_scans = 16

X_90_width = 13.905[us]
X_acq_time = 2.18365952[s]
X_angle = 45[deg]
X_atn = 3[db]
X_pulse = 8.9525[us]
Tri_mode = Off
Dante_preset = FALSE
Initial_wait = 1[s]
Recvr_gain = 40
Relaxation_delay = 5[s]
Repetition_time = 7.18365952[s]
Temp_get = 20.8[degC]

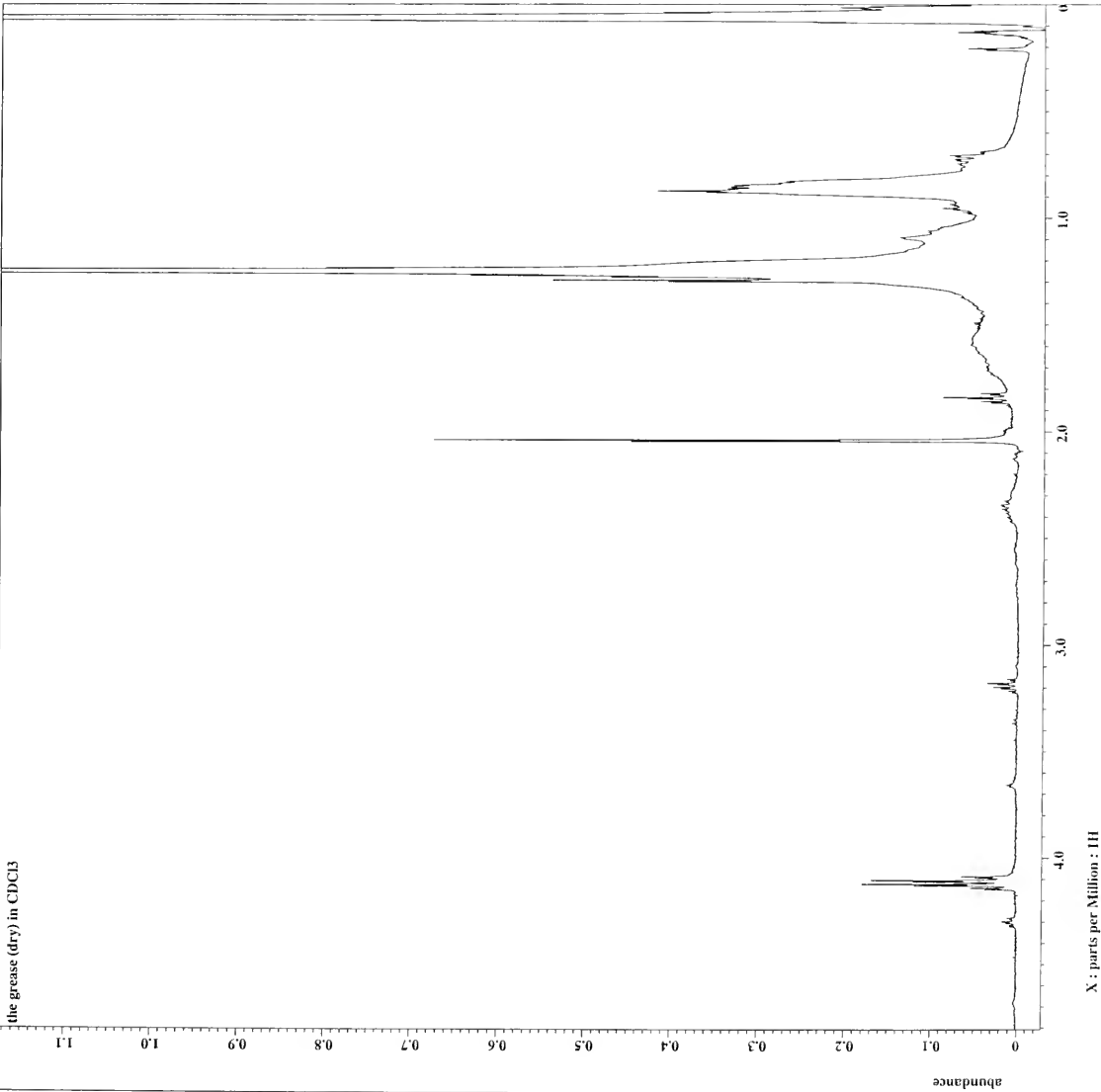


NMR-1



X: parts per Million : 114

6-2119



X : parts per Million : 1H

NMR D-7



```

Filename      = ac-hf-30-18b 1H-3.jdf
Author        = 
Experiment    = single pulse-ex2
Sample_id     = ac-hf-30-18b
Solvent       = CHLOROFORM-D
Creation_time = 8-MAR-2005 11:31:02
Revision_time = 25-APR-2005 14:01:08
Current_time  = 25-APR-2005 14:01:15

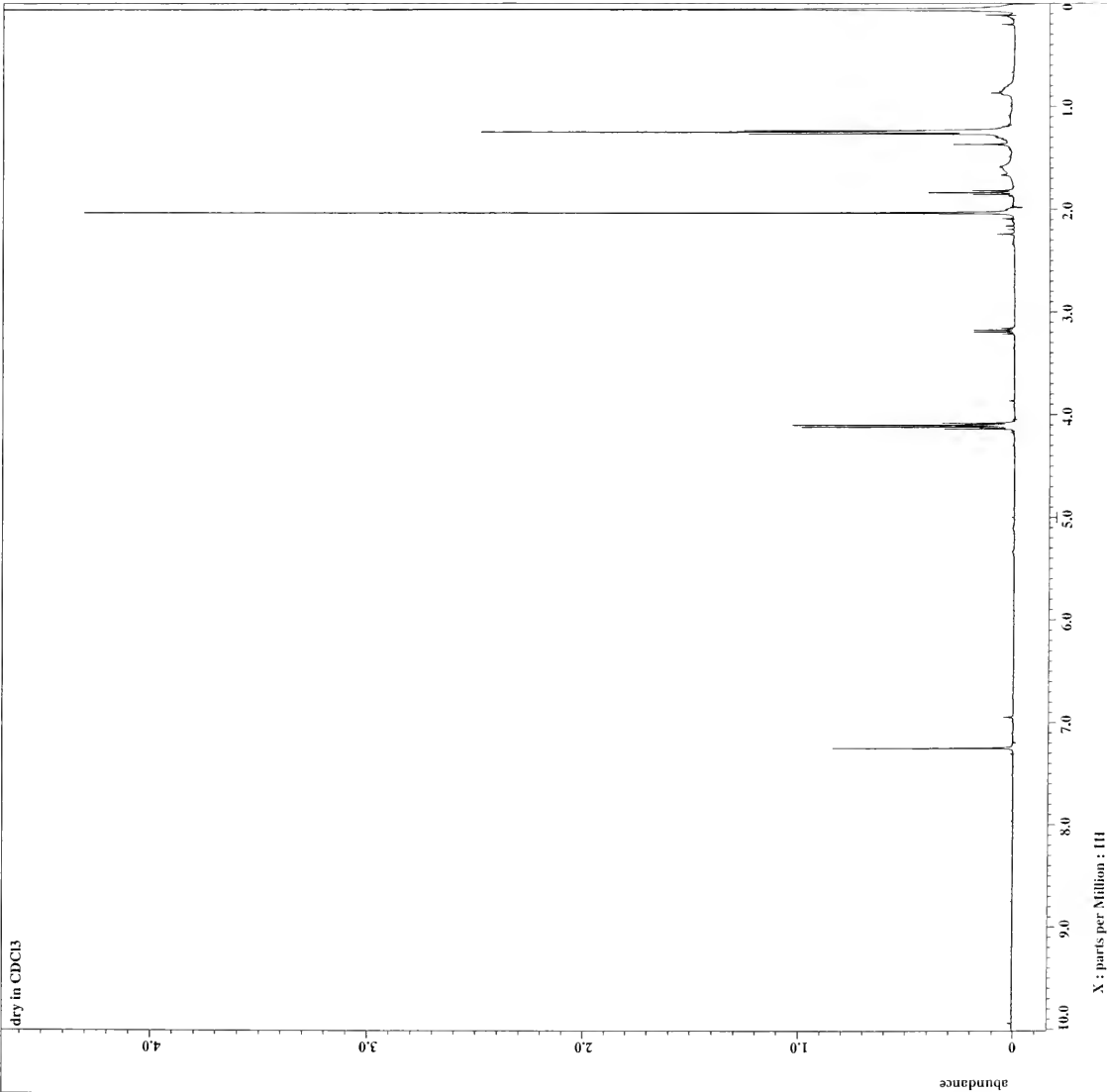
Content
= the grease (dry) in C
Data format  = ID COMPLEX
Dim_size     = 13107
Dim_title    = 1H
Dim_units    = [ppm]
Dimensions   = X
Site         = ECX 400
Spectrometer = DELTA2_NMR

Field_strength = 9.389766 [T] (400 [MHz])
X_acq_duration = 2.18365952 [s]
X_domain       = 1H
X_freq         = 399.78219838 [MHz]
X_offset       = 16384
X_points       = 16384
X_prescans     = 1
X_resolution   = 0.45794685 [Hz]
X_sweep        = 7.5030012 [kHz]
X_domain       = 1H
lrr_freq       = 399.78219838 [MHz]
lrr_offset     = 5 [ppm]
Tri_domain     = 1H
Tri_freq       = 399.78219838 [MHz]
Tri_offset     = 5 [ppm]
C11_offset     = 5 [ppm]
C11_offset     = FALSE
Mod return     = FALSE
Scans          = 8
Total_scans    = 8

X_90_width     = 14.1641 [us]
X_acq_time     = 2.18365952 [s]
X_angle        = 47 [deg]
X_resolution   = 0.45794685 [Hz]
X_pulse        = 7.08205 [us]
lrr_mode       = Off
Tri_mode       = Off
Dante_presat   = FALSE
Initial_wait   = 1 [s]
Recvr_gain     = 38
Relaxation_delay = 5 [s]
Repetition_time = 2.18365952 [s]
Temp_set       = 20.9 [C]

```


dry in CDCl3

X : parts per Million : δ

NMR - 2

```

Filename      = ac-ht-32-23b 1h-2.jdf
Author        = Researcher
Experiment    = ac-ht-32-23b
Sample_id     = ac-ht-32-23b
Solvent       = CHLOROFORM-D
Creation time  = 8-MAR-2005 11:54:19
Revision time  = 25-APR-2005 14:01:35
Current_time   = 25-APR-2005 14:02:24

Content       = dry in CDCl3
Data_format   = 13C107
Dim_title     = 1H
Dim_units     = [ppm]
Dimensions    = X
Site          = ECX 400
Spectrometer  = DELTA2_NMR

Field_strength = 9.389765 [T] (400 [MHz])
X_acq_duration = 2.18365952 [s]
X_domain       = 1H.18365952 [s]
X_freq         = 399.78219838 [MHz]
X_offset       = 5 [ppm]
X_points       = 16384
X_prescans     = 1
X_resolution   = 0.45794685 [Hz]
X_sweep        = 7.5930012 [kHz]
Tri_domain    = 1H
Tri_freq       = 399.78219838 [MHz]
Tri_offset     = 5 [ppm]
Tri_domain     = 1H
Tri_freq       = 399.78219838 [MHz]
Tri_offset     = 5 [ppm]
Clipped        = FALSE
Acq_return     = 8
Scales         = 8
Total_scans    = 8

X_90_width     = 14.1641 [us]
X_acq_time      = 2.18365952 [s]
X_angle         = 45 [deg]
X_atn           = 3 [dB]
X_pulse         = 12.06205 [us]
Tri_pulse       = Off
Tri_mode        = Off
Dante_presat    = FALSE
Initial_wait    = 1 [s]
Recvr_gain      = 40
Relaxation_delay = 5 [s]
Repetition_time = 7.18365952 [s]
Temp_get        = 21.3 [dC]

```



dry in CDCl3

4.0

3.0

2.0

1.0

abundance

4.0

3.0

2.0

1.0

0

X : parts per Million : 1H

NMR - 2



```

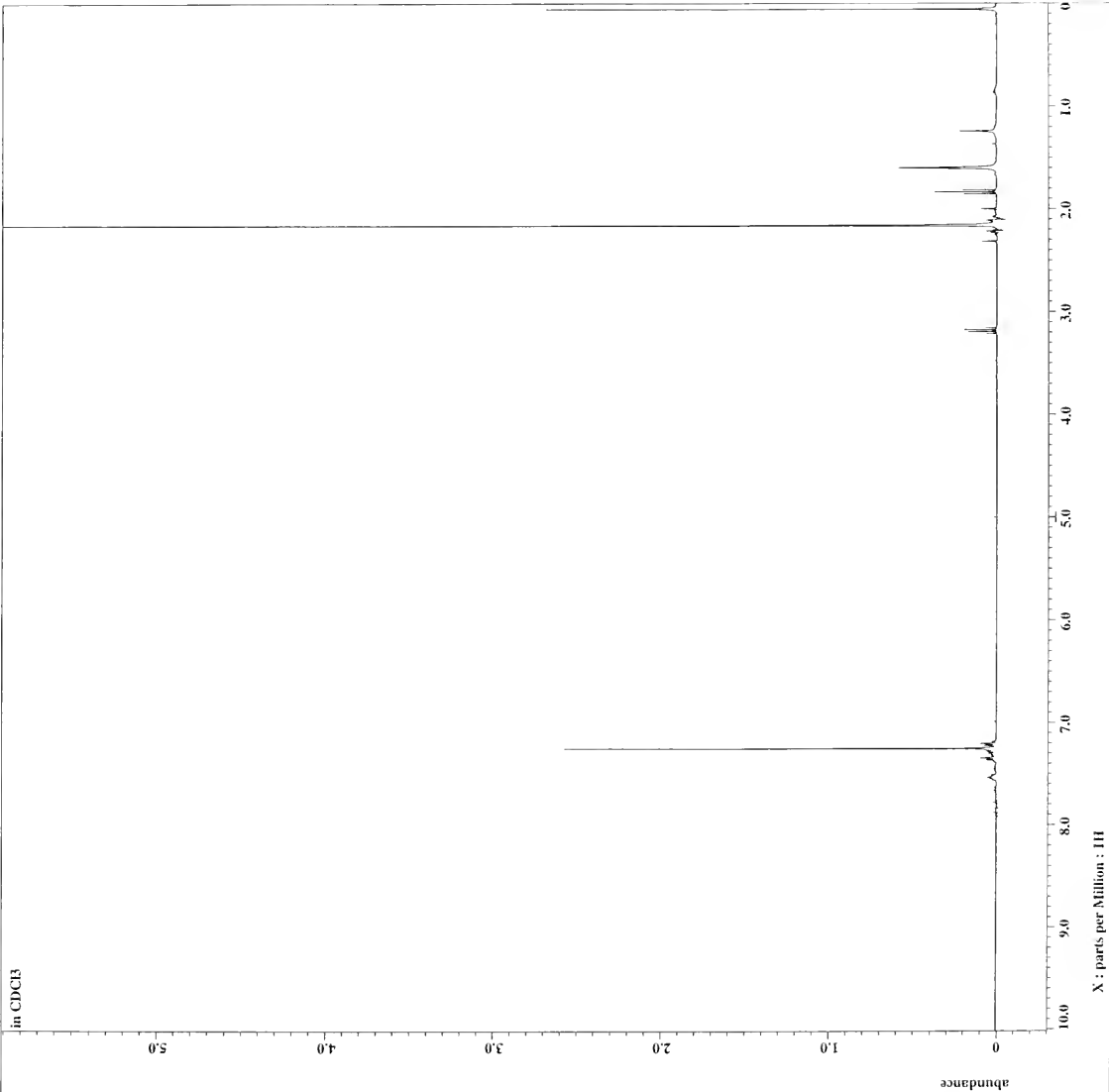
Filename      = ac-hi-32-23b 1h-3.jdf
Author        = Researcher
Experiment     = single pulse.ex2
Sample_id     = CHLORFORM-D
Solvent        = CHLORFORM-D
Creation_time  = 8-MAR-2005 11:54:19
Revision_time  = 25-APR-2005 14:05:59
Current_time   = 25-APR-2005 14:06:03

Content
Data_dir       = dry in CDCl3
Data_format    = 13C NMR
Dim_size       = 1H 107
Dim_title      =
Dim_units      = [ppm]
Dimensions     = X
Site           = ECX 400
Spectrometer   = DELTA2_NMR

Field_strength = 9.389766 [T] (400 [MHz])
X_acq_duration = 2.18365952 [s]
X_domain       = 1H 48365952 [Hz]
X_freq         = 399.78219838 [MHz]
X_offset       = 5 [ppm]
X_points       = 16384
X_prescans     = 1
X_resolution   = 0.45794685 [Hz]
X_sweep        = 1H 3030012 [kHz]
Tri_freq       = 399.78219838 [MHz]
Tri_offset     = 5 [ppm]
Tri_domain     = 1H
Tri_freq       = 399.78219838 [MHz]
Tri_offset     = 5 [ppm]
X_clipped      = FALSE
X_return       = 1
Scans          = 8
Total_scans    = 8

X_90_width     = 14.1641 [us]
X_acq_time     = 2.18365952 [s]
X_angle        = 45 [deg]
X_atn          = 3 [dB]
X_pulse        = 16.26205 [us]
Tri_mode       = Off
Dante_presat   = FALSE
Initial_wait   = 1 [s]
Recvr_gain     = 40
Relaxation_delay = 5 [s]
Repetition_time = 7.18365952 [s]
Temp_get       = 21.3 [dC]

```

NMR-1



```

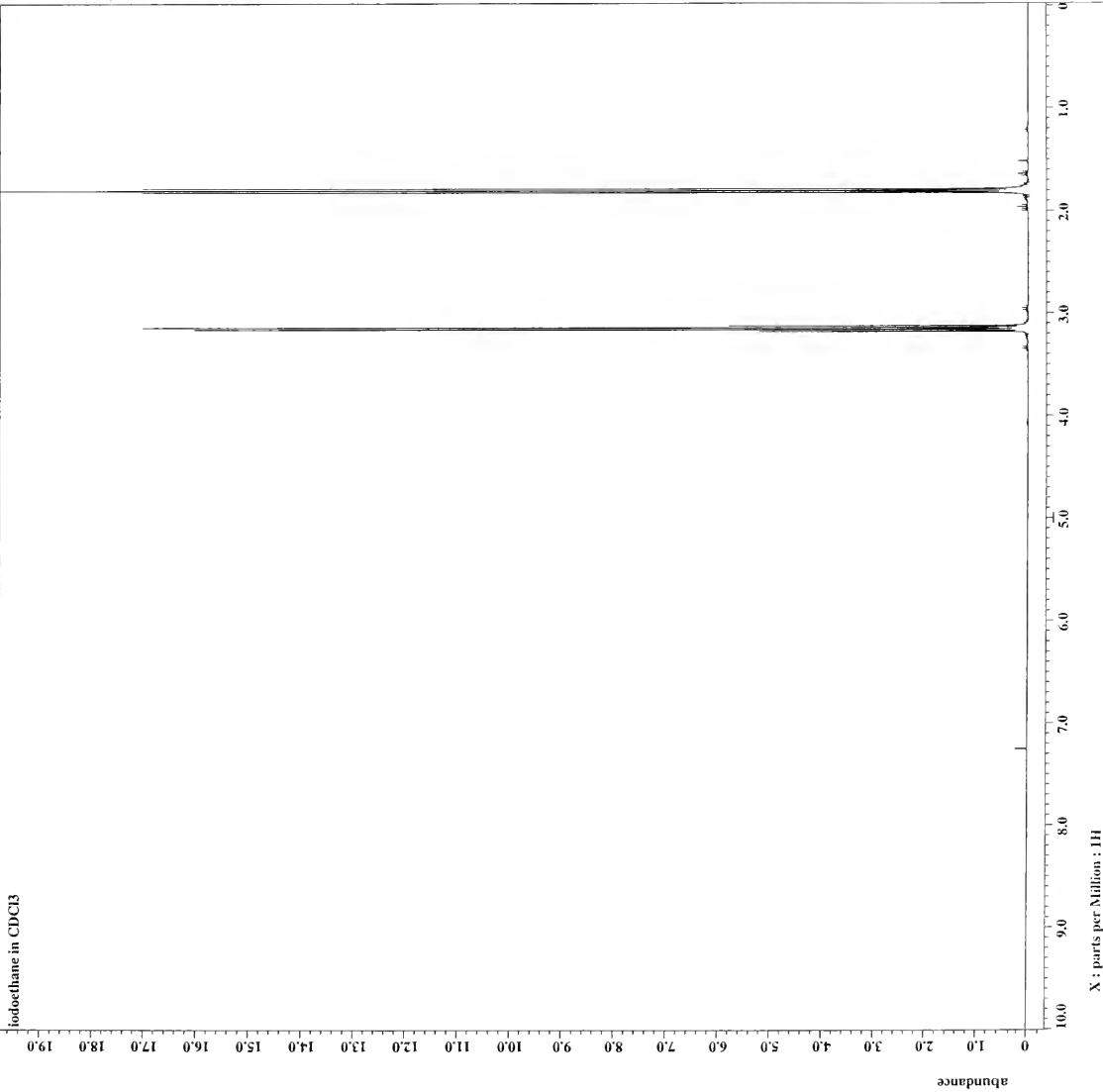
Filename      = ac-ht-34-21 1h-3.fdf
Experiment    = 1hnmrht34
Sample_id     = single.pulse.ex2
Solvent       = ac-ht-34-21
              = CHLOROFORM-D
Creation_time = 29-MAR-2005 14:23:05
Revision_time = 25-APR-2005 14:08:50
Current_time  = 25-APR-2005 14:08:52

Content
  = in CDCl3
Data format  = ID COMPLEX
Dim.size     = 13107
Dim.title    = 1H
Dim.units    = [ppm]
Dimensions   = X
Site         = ECX 400
Spectrometer = DELTA2_NMR

Field strength = 9.389766[T] (400[MHz])
X_acq_duration = 2.18365952[s]
X_domain       = 1H
X_freq         = 399.78219838[MHz]
X_points       = 16384
X_prescans     = 1
X_resolution   = 1.45794685[Hz]
X_sweep        = 7.5030012[kHz]
X_domain       = 1H
Irr_domain     = 399.78219838[MHz]
Irr_freq       = 5[ppm]
Irr_offset     = 1H
Tri_domain     = 399.78219838[MHz]
Tri_freq       = 5[ppm]
Tri_offset     = 1H
C13_prescans   = 1
Mod_return     = FALSE
Scans          = 8
Total_scans    = 8

X_90_width     = 14.1641[us]
X_acq_time     = 2.18365952[s]
X_angle        = 4[deg]
X_p1           = 7.08205[us]
X_pulse        = Off
Irr_mode       = Off
Tri_mode       = FALSE
Dante_preset   = Initial_wait
Initial_wait   = 1[s]
Recvr_gain     = 42
Relaxation_delay = 7.18365952[s]
Relaxation_time = 22[dc]
Temp_get       = 22[dc]

```

```

Filename      = ac-ht-28-18 1h-2.jdf
Author        = Researcher
Experiment     = single_pulse.ex2
Sample_id     = ac-ht-28-18
Solvent        = CHLOROFORM-D
Creation_time  = 15-FEB-2005 15:29:09
Revision_time  = 25-APR-2005 14:11:02
Current_time   = 25-APR-2005 14:11:50

Content       = Iodoethane in CDCl3
Data_format   = ID COMPLEX
Dim_size      = 13107
Dim_title     = 1H
Dim_units     = [ppm]
Dimensions    = X
Site          = ECX 400
Spectrometer  = DELTA2_NMR

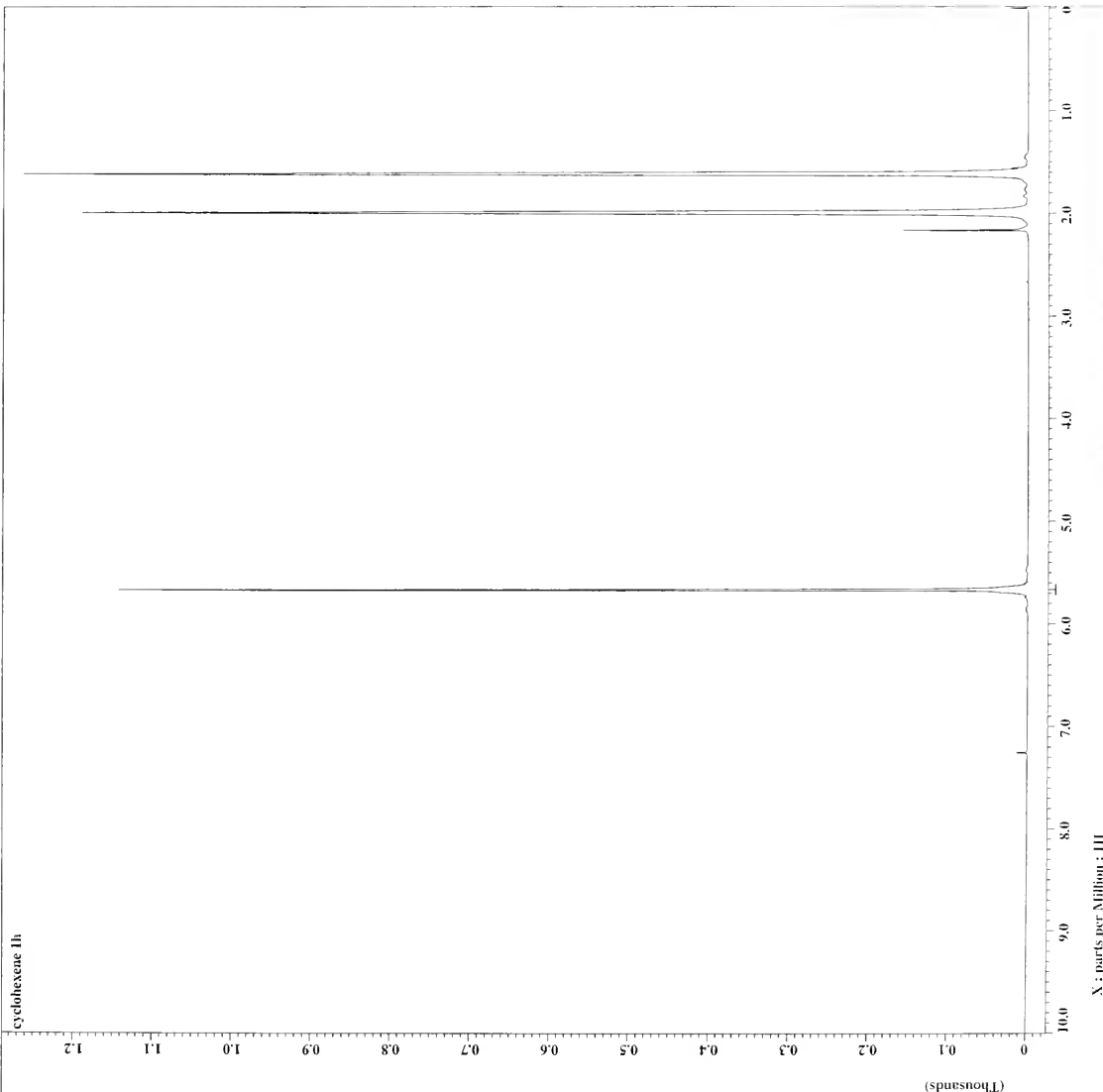
Field_strength = 9.389766[T] (400 [MHz])
X_acq_duration = 2.18103808[s]
X_domain      = 1H
X_freq        = 399.78219838 [MHz]
X_offset      = 5[ppm]
X_points      = 16384
X_prescans    = 0
X_resolution  = 0.45849727 [Hz]
X_sweep       = 7.51201923 [MHz]
X_domain      = 1H
Irr_domain    = 399.78219838 [MHz]
Irr_freq      = 5[ppm]
Irr_offset    = 1
Tri_domain    = 1H
Tri_freq      = 399.78219838 [MHz]
Tri_offset    = 5[ppm]
C1_offset     = 1
Mod_return    = FALSE
Scans         = 8
Total_scans   = 8

X_90_width    = 14.1641[use]
X_acq_time     = 2.18103808[s]
X_angle        = 30[deg]
X_attn         = 3[dB]
X_pulse        = 7.08205[use]
Irr_mode       = Off
Tri_mode       = Off
Dante_presat   = FALSE
Initial_wait   = 1[s]
Recvr_gain     = 28
Relaxation_delay = 7.18103808[s]
Relaxation_time = 20.4[dc]
Temp_get       = 20.4[dc]

```


CYCLOHEXENE

cyclohexene 1h

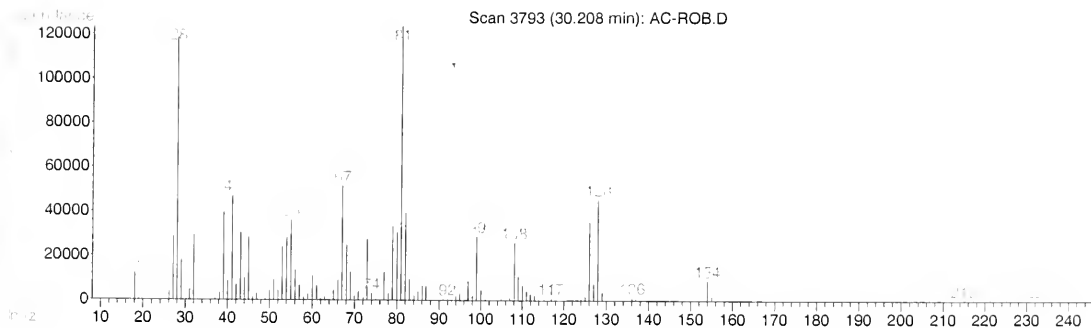
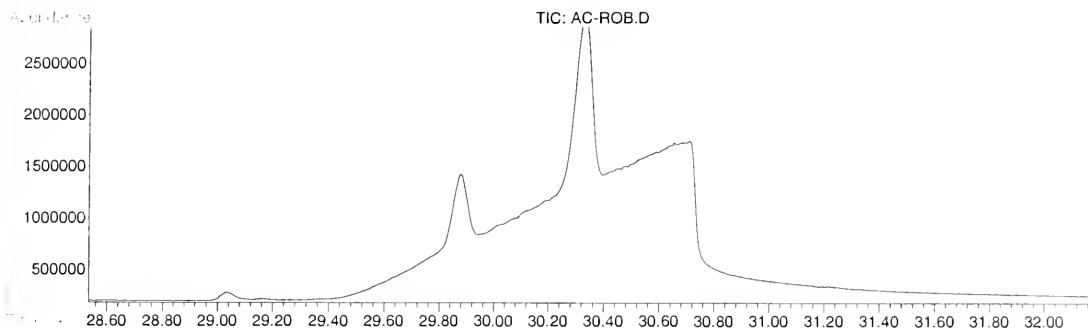


X : parts per Million : 1H

NMR 1-1

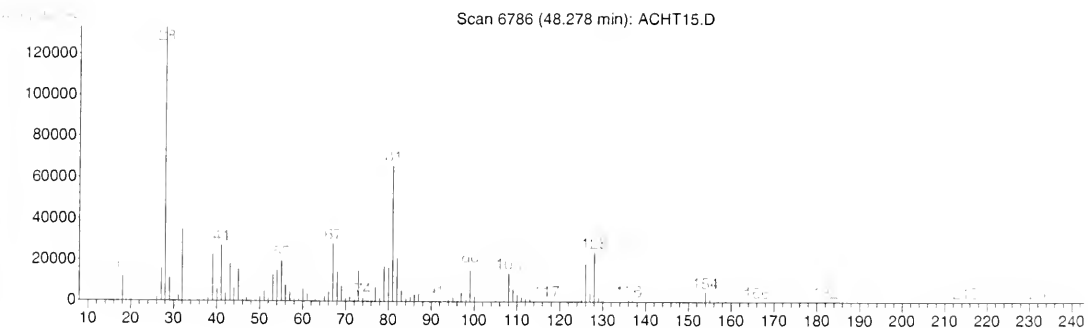
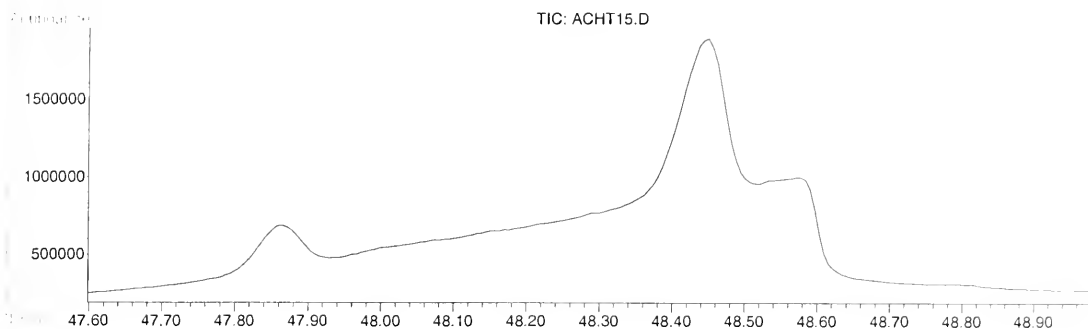
Filename = ac-ht-21-13 1h-3.jdf
 Author = SRC Researchers
 Experiment = single_pulse.ex2
 Sample_id = ac-ht-21-13
 Solvent = CHLOROFORM-D
 = 30-NOV-2004 14:27:47
 Creation_time = 25-APR-2005 13:47:30
 Current_time = 25-APR-2005 13:47:37
 Content = cyclohexene 1h
 Data_format = ID COMPLEX
 Dim_size = 13107
 Dim_title = 1H
 Dim_units = [ppm]
 Dimensions =
 Site = ECX 400
 Spectrometer = DELTA2_NMR
 Field_strength = 9.389766[T] (400 [MHz]
 X_acq_duration = 2.18365952[s]
 X_domain = 189.78219838 [MHz]
 X_offset = 5 [ppm]
 X_points = 16384
 X_prescans = 1
 X_resolution = 0.45794685 [Hz]
 X_sweep = 7.5030012 [Hz]
 Irr_domain = 189.78219838 [MHz]
 Irr_freq = 5 [ppm]
 Irr_offset = 1H
 Tri_domain = 189.78219838 [MHz]
 Tri_freq = 5 [ppm]
 Tri_offset = 5 [ppm]
 Mod_return = 1
 Scans = 8
 Total_scans = 8
 X_90_width = 13.905 [us]
 X_acq_time = 2.18365952 [s]
 X_angle = 45 [deg]
 X_atn = 3 [dB]
 X_pulse = 6.9525 [us]
 Irr_mode = off
 Irr_offset = 0
 Irr_presat = FALSE
 Initial_wait = 1 [s]
 Recvr_gain = 22
 Relaxation_delay = 5 [s]
 Repetition_time = 7.18365952 [s]
 Temp_get = 20.7 [dC]

File : C:\HPCHEM\1\DATA\AC-ROB.D
Operator : RGranger
Acquired : 28 Oct 2004 12:26 using AcqMethod OXYLATE
Instrument : GC/MS Ins
Sample Name: Ana's stuff
Misc Info : Trouble shooting
Vial Number: 1



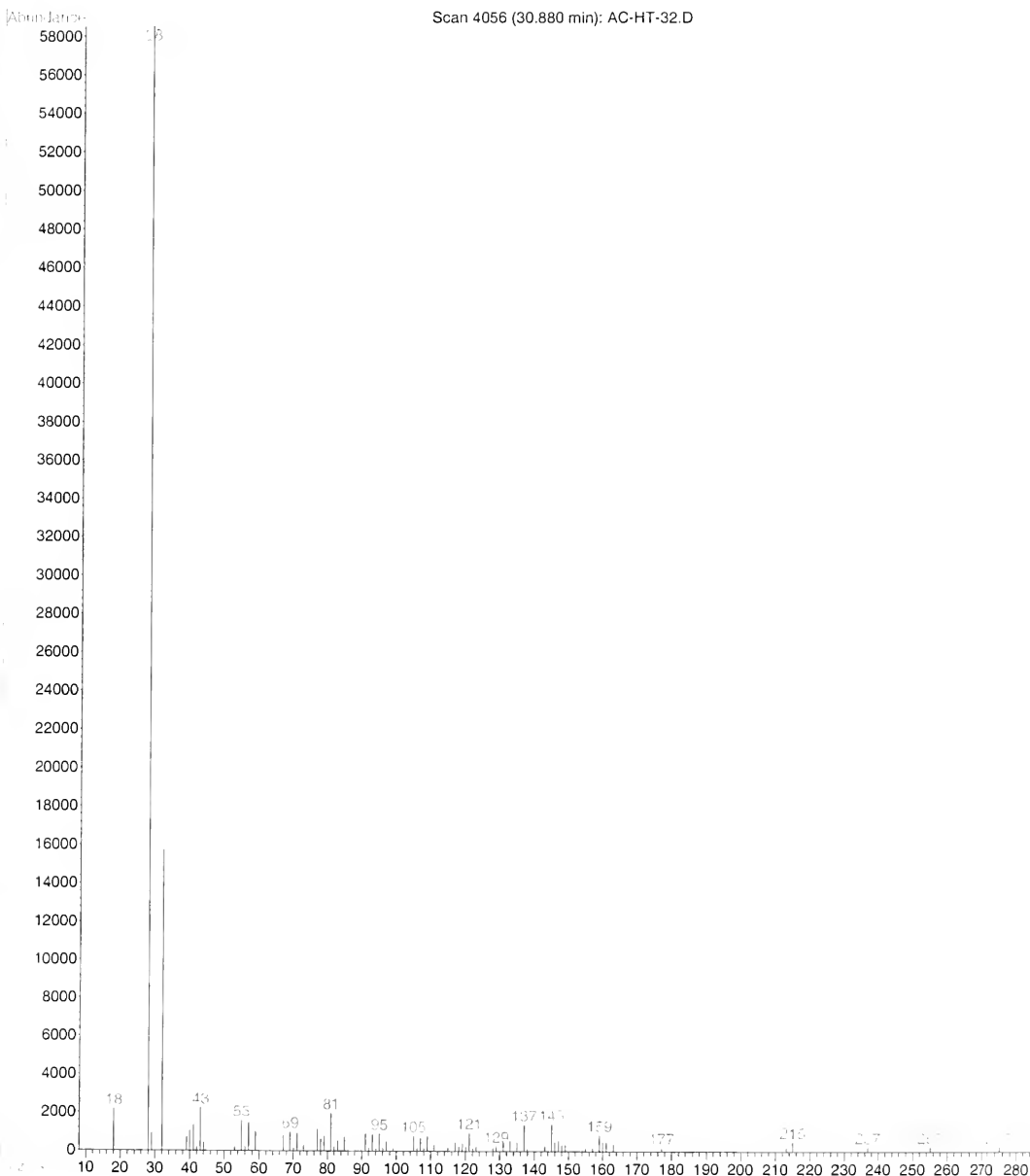
GC/MS-1

File : C:\HPCHEM\1\DATA\CIRIC\ACHT15.D
Operator : Ana Ciric
Acquired : 9 Nov 2004 17:24 using AcqMethod OXYLATE
Instrument : GC/MS Ins
Sample Name: Ester of Cat Electrolysis
Misc Info : Ethanol
Vial Number: 1



GC/MS-2

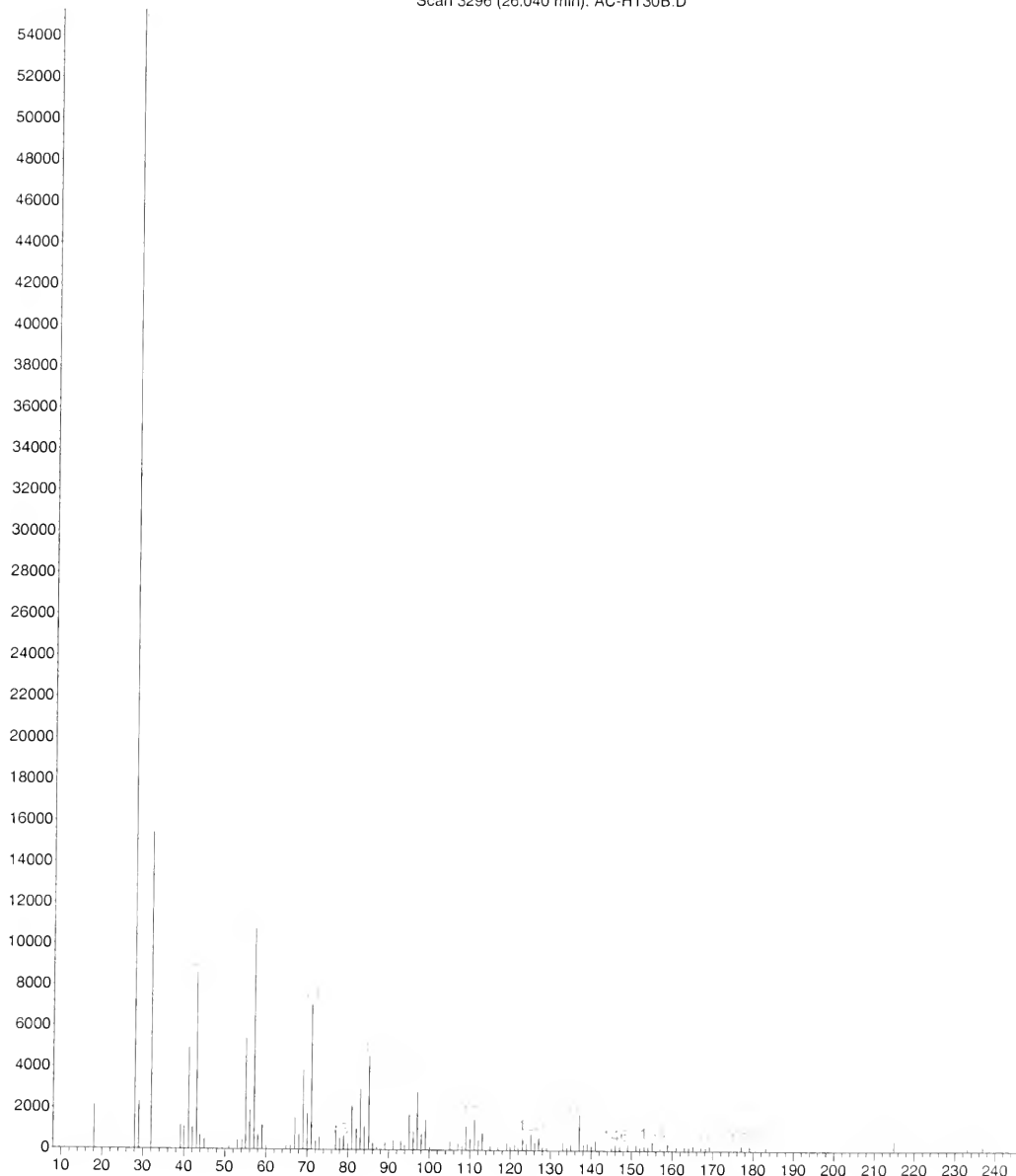
File : C:\HPCHEM\1\DATA\CIRIC\AC-HT-32.D
Operator : Ana Ciric
Acquired : 1 Mar 2005 15:49 using AcqMethod OXYLATE1
Instrument : GC/MS Ins
Sample Name: checking the esterification process
Misc Info : diethyloxylate in EtOAc
Vial Number: 1



GC/MS - 3

File : C:\HPCHEM\1\DATA\CIRIC\AC-HT30B.D
Operator : Ana Ciric
Acquired : 27 Feb 2005 18:18 using AcqMethod OXYLATE1
Instrument : GC/MS Ins
Sample Name: the grease in CDCl3
Misc Info : see NMR and IR
Vial Number: 1

Scan 3296 (26.040 min): AC-HT30B.D



GC/MS - 4

2723 3477 6

05/31/06

MFB







